FACULDADE DE ENGENHARIA DA UNIVERSIDADE DO PORTO

Pressure Sensor Automatic Calibration System

Vasco André Ribeiro da Silva Gonçalves

Mestrado em Engenharia Eletrotécnica e de Computadores

Supervisor: Prof. Dr. José Carlos dos Santos Alves

July 30, 2023

Resumo

A ausência ou diferença de membros, seja por amputação ou deformação congénita destes, afeta significativamente a qualidade de vida de inúmeras pessoas em todo o mundo. Com o objetivo de melhorar o nível de vida das pessoas com ausência ou diferença de membros, próteses são frequentemente utilizadas. No caso particular de ausência ou diferença dos membros inferiores, a utilização de próteses permite a estas pessoas restaurar mobilidade e recuperar independência. O ajuste correto de uma prótese é crucial, uma vez que tem um enorme impacto no conforto, no equilíbrio e nas capacidades funcionais do membro protésico.

O processo de ajuste de uma prótese de membros inferiores é um procedimento demorado e iterativo e altamente dependente no feedback dos pacientes. Para ajudar neste processo, várias soluções têm sido desenvolvidas para avaliar o ajuste dos encaixes, ou *sockets*, das próteses, ou seja, as interfaces entre os membros residuais e os componentes protésicos. Um desses sistemas é o sistema INSIGHT™, desenvolvido pela Adapttech®. Este sistema utiliza um conjunto de fitas com sensores de pressão que são colocadas entre o encaixe da prótese e o membro residual do paciente. Estas tiras de sensores incorporam *Force-Sensing Resistors*, que requerem calibração para leituras de pressão precisas e fiáveis.

Esta dissertação tem como objetivo investigar e melhorar o processo de calibração dos *Force-Sensing Resistors* e desenvolver um novo sistema de calibração automático. O principal objetivo deste sistema é reduzir o tempo de processamento do operador. Isto permite uma utilização mais eficiente do tempo do operador e assegura uma leitura fiável e precisa da pressão. Melhorando o processo de calibração e minimizando o envolvimento do operador, o novo sistema de calibração pode possibilitar um desenvolvimento mais rápido do sistema. Consequentemente, o sistema INSIGHT™ melhora a sua disponibilidade e fiabilidade, beneficiando pacientes em todo o mundo.

O novo Sistema de Calibração Automática de Sensores de Pressão foi desenvolvido usando a linguagem de programação Python e os aspetos fundamentais do seu desenvolvimento são descritos nesta dissertação.

Abstract

Limb loss or limb difference, either by amputation or congenital deformation, significantly affects the quality of life for numerous individuals globally. With the goal of enhancing the standard of living of people with limb loss or limb difference, prosthesis are frequently prescribed. In the particular case of absence or difference of lower limbs, the use of prosthesis enables patients to restore mobility and regain independence. The correct fit of a prosthesis is crucial as it has an immense impact on comfort, balance and functional capabilities of the prosthetic limb.

The fitting process of lower limb prosthesis is a time consuming and iterative procedure that is highly dependent on the feedback of patients. To aid in this process, various solutions have been developed to assess the fit of prosthetic sockets which are the interfaces between the residual limbs and the prosthetic components. One such system is the INSIGHT™, developed by Adapttech®, this system uses an array of pressure sensor strips that are placed between the prosthetic socket and the residual limb of the patient. These sensor strips incorporate Force-Sensing Resistors, which require calibration for accurate and reliable pressure readings.

This dissertation aims to investigate and enhance the calibration process of Force-Sensing Resistors and develop a new automatic calibration system. The primary objective of this system is to reduce the operator processing time. This allows for a more efficient use of operator time and ensures a reliable and precise pressure reading. By improving the calibration process and minimizing the involvement of the operator, the new calibration system can offer faster throughput. Consequently the INSIGHT™ system improves its availability and reliability benefiting patients worldwide.

The new Pressure Sensor Automatic Calibration System was develop using Python programming language and fundamental aspects of its development are described in this dissertation.

Agradecimentos

Em primeiro lugar, gostaria de agradecer à Adapttech® por me ter proporcionado a incrível oportunidade de fazer parte deste projeto e à sua equipa por me ter acolhido de forma tão calorosa. Em especial queria agradecer ao meu Supervisor Eng. José Rafael Silva por todo o apoio, conhecimento, disponibilidade e importantes momentos de descontração, ao Eng. Sérgio Silva pelo apoio e ajuda, e à equipa de Embedded Systems por todo o conhecimento, conselhos e contribuições para o Capítulo 6.

Ao meu orientador, Professor José Carlos Alves por toda a orientação e ajuda disponibilizada.

Aos amigos que fiz durante o curso, um obrigado por todos os momentos que passamos juntos, por toda a disponibilidade para ajudar e por todos os projetos que fomos partilhando. Assim como aos amigos que fiz durante toda a vida, um enorme obrigado por toda a amizade, companhia, apoio, gargalhadas e experiências que partilhamos.

A toda a minha família, pelo apoio e por sempre acreditarem em mim, em especial aos meus pais que sempre valorizaram e investiram na minha educação, e à minha avó.

Sem a ajuda de todas estas pessoas não estaria a terminar esta etapa com sucesso. A todos, o meu mais profundo obrigado.

Vasco André Gonçalves

“We live on an island surrounded.
by a sea of ignorance. As our
island of knowledge grows, so does
the shore of our ignorance”

John Archibald Wheeler

Contents

List of Figures

List of Tables

List of Abbreviations

ADC	Analog-to-Digital Converter
APP	Application
ASCII	American Standard Code for Information Interchange
CAD	Computer-Aided Design
CAM	Computer-Aided Manufacturing
CLI	Command Line Interface
CSV	Comma-Separated Values file
EEPROM	Electrically Erasable Programmable Read-Only Memory
EXE	Executable file
FBG	Fiber Bragg Grating
FO	Fiber Optics
FOS	Fiber Optic Sensor
FPC	Flexible Printed Circuit
FSR	Force-Sensing Resistors
GUI	Graphical User Interface
IC	Integrated Circuits
IDE	Integrated Development Environment
iOS	iPhone Operating System
ISP	In-System Programming
LED	Light-Emitting Diode
NAS	Network-attached storage
O&P	Orthotic and Prosthetic
PCB	Printed Circuit Board
R&D	Research and Development
ROM	Read-only Memory
SPI	Serial Peripheral Interface
USA	United States of America
USB	Universal Serial Bus

Chapter 1

Introduction

Although there may be many causes for limb loss and limb difference, amputation of various etiologies is the most widely studied and common, worth particularizing. In the USA alone, in the year of 2005 there were an estimate of 1.6 million amputees. This number is expected to double by 2050 [1]. The same study shows that dysvascular diseases account for approximately 54% of the prevalent cases and of those over two thirds have a comorbid *diabetes mellitus*. Trauma accounts for almost 45% of the cases, and the remaining less than 2% are related to cancer. Of all the people that underwent an amputation it is estimated that lower limb amputees constitute 65% of the cases and that almost 61% of this amputations are considered major, meaning excluding toe amputation. Lower limb amputation can be classified in 5 major groups depending of the point of removal (Figure 1.1).

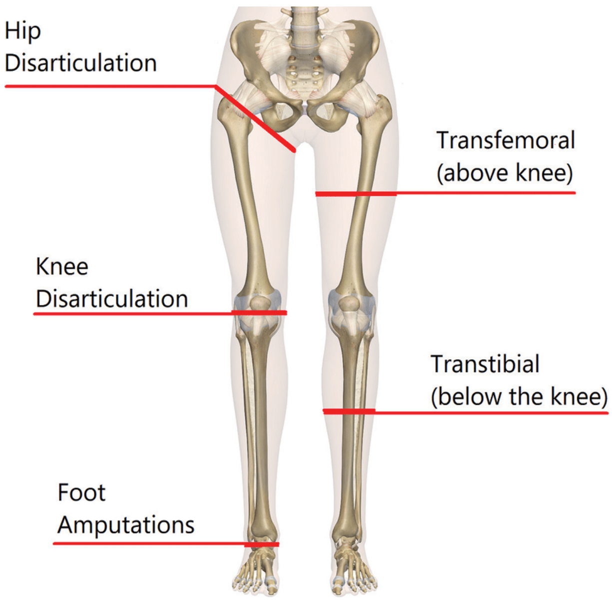

Figure 1.1: Level of lower limb amputation [2]

Hip disarticulation and knee disarticulation (or through knee) consist of the removal of the lower limb at the joints (hip and knee respectively). Transtibial and transfemoral are the most common amputations and include separation along the length of the bone (tibia or femur respectively). Lastly, foot amputation considers all amputations (at the joints or not) performed bellow or at the ankle level such as mid-tarsal, Boyds, Symes along with others. [3]

Such interventions strongly impact the patients' lives in almost all aspects of their professional, social and personal life. Be that as it may, they are deemed indispensable as they are linked with life threatening situations and as such aim to improve and prolong the life of patients.

Oftentimes, prostheses are used to increase independence, mobility and overall well-being of patients. For lower limb amputees, the process of acquiring a new, well-fitting prosthesis is discernibly outdated, due to the lack of use of technology and a "trial and error" approach.

Figure 1.2: Parts of transfemoral prosthesis [4]

Lower limb prostheses are usually comprised of a foot, a pylon, a knee system (only in the case of above knee amputees) and a socket (Figure 1.2). The socket is the interface between the residual limb of the patient, also referred to as stump, and the prosthetic components.

The correct fitting of the socket is crucial on account of the fact that a poorly fitted prosthetic leg can cause discomfort and pain that if not corrected in due time can lead to frustration and ulcers. The latter is a common problem with amputees that can ultimately result in the inability to temporarily wear the prosthesis and if left untreated cause permanent damages. In lower limb amputees this might mean reducing their mobility, independence and quality of life. A socket is considered well fitted if it is comfortable for the user and the interfacial pressure is evenly distributed, bearing in mind that there are pressure-sensitive and pressure-tolerant areas in residual limbs that must be loaded differently to ensure proper fit.

The process of fitting the socket is very complex and challenging due to the uniqueness and complexity of the residual limb of each prosthesis user [5]. It also lacks the help of technology, so it is based on trial and error.

Figure 1.3: Typical socket fitting workflow [6]

The traditional process (Figure 1.3) starts by creating a plaster cast of the remainder of the limb, then a positive model of the limb is made and modified to better match the patient's residual limb, a socket is then formed around the model. This socket now needs to be fitted to the patient. During the following visits to the Orthotics and Prosthetics Clinic the patients need to try on the socket and give feedback. Then adjustments to the socket are made and the process is repeated until reached a satisfactory result. The entire process requires, typically, from 7 to 18 visits. This approach is highly influenced by the patient's ability to give useful feedback as well as by the experience of the clinician. Such lengthy process and the psychological factors related are bound to generate frustration on a significant number of patients.

Moreover the same patient can undergo this process several times in their lifetime. Loss or damage to the socket or whole prosthesis are a common reason but the list extends to medical reasons for example development of ulcers and the most common weigh oscillations.

Despite some studies there are still few commercially available solutions focusing on aiding the fitting process. Aiming to improve this process, Adapttech® has developed the INSIGHT™ system for measuring the pressure distribution inside the socket and help the process of adjusting the socket. This system is expected to halve the time of the fitting process, allowing a faster return to normal life, a more accurate fitting socket, reducing the pain, discomfort, or risk of more serious complications while also enabling a more active life due to better fit. It also improves the reliability of the socket because it is less influenced by the experience of the clinician.

1.1 Objectives

The solution presented by Adapttech® uses thin strips with several pressure sensors built with Force-Sensing Resistors (FSR). These FSR sensors need to be calibrated and tested before the product can be used. The goal of the dissertation is to automate the calibration process of the pressure sensors strips used by Adapttech® INSIGHT™

As of this moment, the sensors are placed under a pneumatic press and there is a need for a worker to manually input the data collected by the sensors into a calibration app while cycling the pressure applied to the sensor.

The sensor strips consist of multiple pressure sensors and a PCB that interprets the sensor signals, store calibration information for each sensor, and communicates with the wearable device. At this time there is a separated process responsible for flashing the firmware of the components present on the pcb.

It is expected that the solution that eliminates the need for manual intervention, reduces calibration time, and improves the accuracy of the calibration process. By automating the calibration and incorporating the flashing process, the solution will allow individuals to focus on more valuable tasks, while also accelerating the availability of the system for patients.

1.2 Motivation

With the predicted increase in the number of people with limb loss or limb difference, achieving a precise and comfortable prosthetic socket fit is crucial for enhancing their quality of life. I believe that by expediting the calibration process while making it more independent and reliable, my work along with Adapttech® can have an impact on those struggling to get a fitting lower-limb prosthesis, enabling them to experience greater independence, functionality, and satisfaction in their daily lives.

1.3 Document Structure

This dissertation is divided in eight chapters. This first chapter serves as an introduction of limb loss and limb difference, the difficulties this patients currently have to withstand and the underlying motivation for this dissertation.

Chapter 2 describes the INSIGHT™ system developed by Adapttech® and other solutions that are relevant for this dissertation.

Chapter 3 elaborates on the current state of the art for pressure sensors as well as calibration methods for Force-Sensing Resistors.

Chapter 4 presents the main characteristics of the sensors used by the INSIGHT™ system and contextualizes the manual system previously implemented describing its components, workflow and negative aspects.

Chapter 5 elaborates on the development of the automatic system and its structure.

Chapter 6 discusses complementary work that was done for the enrichment of this dissertation.

Chapter 7 compares the automatic calibration system with the manual system and further discusses the results achieved.

Lastly, Chapter 8 presents the conclusion of this dissertation as well as outlining improvements for the system.

Chapter 2

Related Work

In this chapter the INSIGHT™ product line, developed by Adapttech® is presented. Furthermore, different solutions or solutions that use relevant technology are discussed.

2.1 Adapttech® INSIGHT™

Adapttech® is a biomedical innovation company that brings new smart technologies to the O&P market with the goal of empowering clinicians with better socket fitting and monitoring methods to improve the quality of life for people with lower-limb loss while providing a more efficient process for prosthetists [6]. As mentioned before Adapttech® has developed the INSIGHT™ system with the *motto "A better fit for a better life"*. This innovative system aims to revolutionize the socket fitting process by enhancing its speed, reliability, and objectivity. Currently there are three commercially available products as part of the INSIGHT™ range: INSIGHT™ Sense, INSIGHT™ Digitizer and INSIGHT™ Pro.

2.1.1 INSIGHT™ Sense

INSIGHT™ Sense is a portable and stand alone system for real-time socket pressure measurement that tracks pressure data, contextualizing it with the patient's gait phases. It is comprised of a wearable device that connects to 4 to 8 sensitized strips that must be placed on predetermined positions inside the prosthetic socket. A generic 3D model of the socket is generated based on measurements in key anatomical points and the information gathered by the sensors is displayed on an iOS App.

The INSIGHT™ Sensors (Figure 2.1a) are thin and flexible sensitized strips that measure the pressure between the residual limb of a patient and the prosthetic socket. Each sensor strip is composed of 4, 6, or 8 pressure sensors distributed along its length.

The INSIGHT™ Wearable (Figure 2.1b) is a flexible wearable device that the sensors connect to, providing real-time evaluation of bio-data for clinicians to ensure optimal prosthetic fit and monitor the rehabilitation process of a patient.

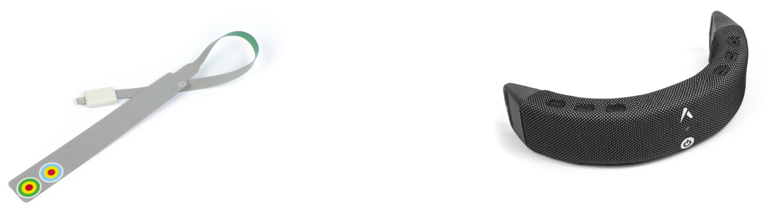

(a) (b)

Figure 2.1: (**a**) INSIGHT™ Sensors, (**b**) INSIGHT™ Wearable [6]

The INSIGHT™ App (Figure 2.2) is connected with the Wearable for gathering and translating data. It conveys an optimized solution to the technician, efficiently ensuring an appropriate prosthetic fit for each individual patient.

The patient must then test the prosthetic socket executing static and dynamic tests. The pressure distribution data is then displayed on the INSIGHT™ App using the previously generated generic socket. The clinician can analyze and record real time pressure data to assess if there is an even load distribution, which takes into account the necessities pressure-tolerant and pressure-sensitive areas, between the patient's stump and the socket and decide which, if any, adjustments are necessary. It is also possible to analyze the pressure distribution in the different gait phases.

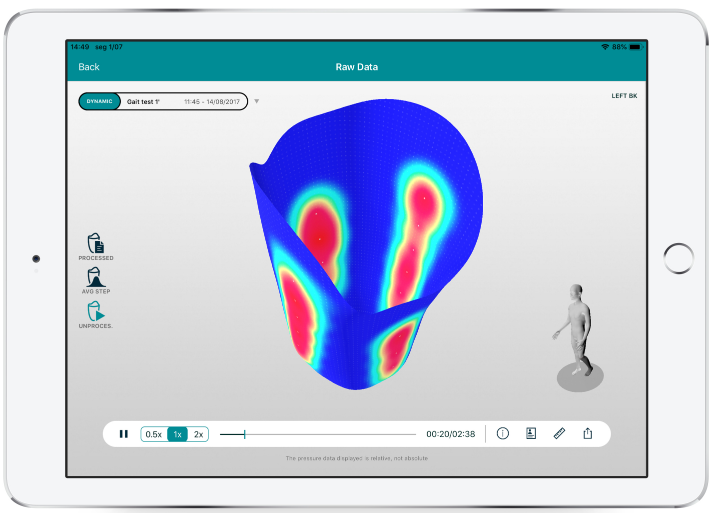

Figure 2.2: INSIGHT™ App displaying the distribution of pressure inside a socket [6]

The data collected can be viewed during or after the consultation and even on another visit. This gives the prosthetist the opportunity to identify problems more quickly and efficiently.

INSIGHT™ Sense is targeted for smaller clinics, clinicians who work remotely, and practices that regularly work with prosthetist residents.

2.1.2 INSIGHT™ Digitizer

Figure 2.3: Adapttech® INSIGHT™ Digitizer (height: 1.80m) [6]

INSIGHT™ Digitizer is a digital scanner that creates 3D models, in STL format, of sockets and plaster casts used as a guide for developing a test socket. The socket or plaster cast is inserted through the door on the front and a 3D copy is created. By creating a digital copy of the socket, the system allows clinics to significantly reduce storage space normally used for physical copies. The 3D models can be used to quickly replace a lost or damaged socket by 3D printing or carving, or even be manipulated to adapt to weight fluctuations. Also, prosthesis users often require additional prosthetic devices for their various needs. Creating a swimming prosthesis or a prosthesis dedicated to physical activity will require the duplication of the prosthetic socket. Without means to do this automatically, the prosthesis user will have to undergo the manual, iterative process of socket fitting over again every time they require an additional prosthetic device. Another benefit is integration with the CAD/CAM workflow.

INSIGHT™ Digitizer is targeted at Central Fabrication, large clinic groups and any clinics using CAD/CAM software to carve or 3D print sockets.

2.1.3 INSIGHT™ Pro

INSIGHT™ Pro is an ensemble of the two systems. The technicians start by freely placing the sensors inside the socket. The digitizer identifies and precisely locates each sensor. On the INSIGHT™ app it is possible to analyze the pressure distribution overlapped on a accurate 3D model of the socket. This system combines the upsides aforementioned, empowering clinics to store information relative to pressure distribution on different iterations and a more precise outcome.

Figure 2.4: Adapttech® INSIGHT™ Pro (not to scale) [6]

2.1.4 General considerations for INSIGHT™ Sense and INSIGHT™ Pro

Focusing on INSIGHT™ Sense and INSIGHT™ Pro as these systems utilize the sensors strips that are the scope of this dissertation and are the systems that aim to evaluate the pressure distribution on the prosthesis.

On any given sensor strip there are multiple FSR sensors. These FSR individually send information regarding the pressure distribution on their surface. It is important to note that the goal is to compare the pressure along all the sensors and not to have an absolute value. The data is then colour coded and presented on the INSIGHT™ App Figure 2.5. As can be seen, the App presents a 3D socket, which, in the case of INSIGHT™ Sense is a generic model that roughly matches the patient's. For INSIGHT™ Pro it is a accurate representation of the socket. Both 3D models are presented with the pressure distribution displayed on their surface. Each line of dots represents a strip and each dot a sensor. Some expected results are shown in Figure 2.5. Please consider that red does not necessarily mean unfavorable fit but rather a considerable higher pressure than the point of lowest pressure or the highest value.

This data can be viewed dynamically and utilized to evaluate patient's gait and determine if there are aspects that need to be addressed that would not become noticeable if merely considering static data.

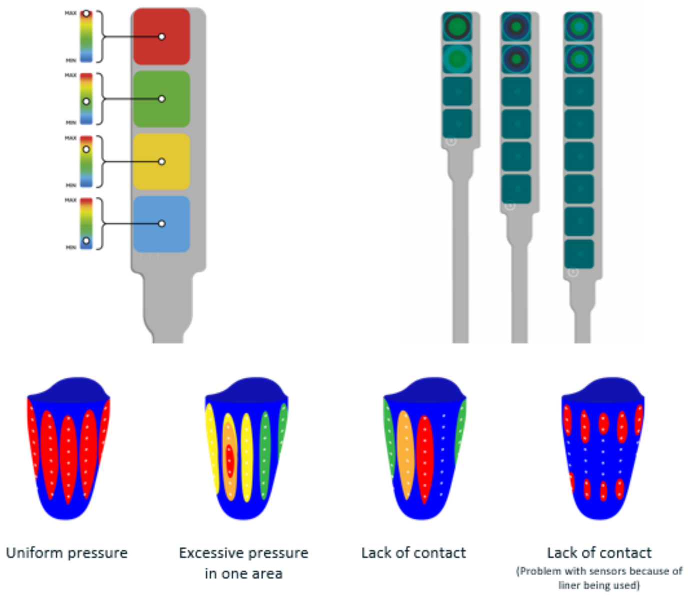

Figure 2.5: Data presented on INSIGHT™ App [6]

With INSIGHT™ Pro, the traditional fitting workflow is improved (Figure 1.3) becoming less subjective, more precise and less impacting, as evident on Figure 2.6 .

Figure 2.6: INSIGHT™ Pro workflow [6]

2.2 Current Solutions and Similar technologies

Presently there are still few commercially available alternatives, with the exception of Adapttech® that presents the only solution that combines the ability to judge the fit while at the same time promoting CAD and CAM manipulation. Nonetheless, this section will elaborate on some solutions that have impact on the fitting process or that utilize technology that can be adapted.

2.2.1 Liners

Figure 2.7: Prosthetic Liner [7]

Using a prosthetic liner (Figure 2.7) can be seen as a strategy to improve prosthetic socket fit, enhance comfort, and solve some problems related to pressure distribution. It is a low tech, traditional approach, comprising a protective layer worn over the residual limb, made in a range of shock absorbing material and various thickness. They can be designed considering many characteristics, uses and special features such as antibacterial features or non-stick treatments to name a few [8]. Common materials used are silicone, polyurethane and copolymer.

This approach presents some advantages such as reduced chafing, ability to adapt to changes of the residual limb and a lower cost. Unfortunately it does not improve the fit nor the fitting process. It can be viewed as means of improving a well fitted socket.

2.2.2 Tekscan

Tekscan is specialized in Pressure Mapping, Force Measurements and Tactile Sensors. They present two relevant systems ,(Figure 2.8): F-scan (on the left) and F-socket (on the right), both are composed of a matrix of pressure sensors that measure pressure distribution. On one hand, F-scan is an insole worn inside a shoe providing gait analysis and information that can be used for medical purposes, R&D or elite athletes. On the other hand F-socket purpose is to improve design, fit and function of prosthesis and is shaped to closely approximate the curvature of the stump. This

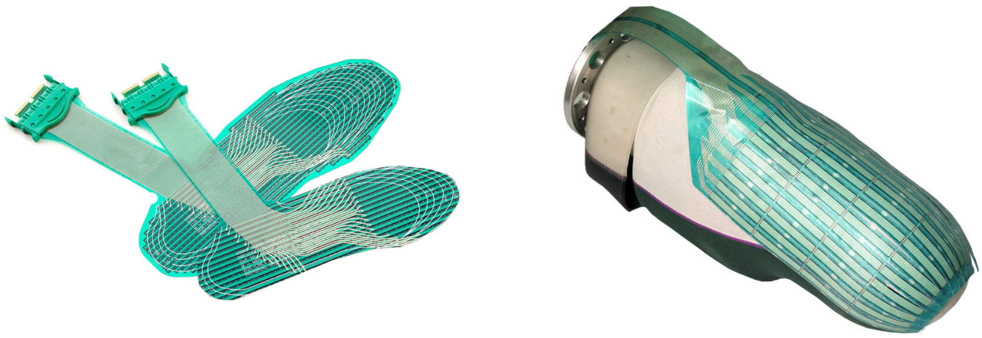

Figure 2.8: Tekscan F-scan and F-socket [9] [10]

approach has the advantage of a very high resolution due to the high number of sensors. Nevertheless, it has its drawbacks such as being outdated and having no information on the real socket, having the pressure information displayed on a rectangular area, without showing data regarding sensor position in relation to the prosthetic device, nor enabling to precisely locate points of higher pressure.

Chapter 3

State-of-the-Art

This chapter expands on the current State-of-the-Art for pressure sensors as well as methodologies for calibration and characterisation.

3.1 Force Sensors

To evaluate the pressure distribution inside a socket it is important to quantify the force exerted on different parts of it. For that reason the most common force sensors presently available are studied.

There have been numerous studies made in the last 50 years on techniques for measuring the stress within prosthetic sockets to judge and improve socket quality, as described on [5], using technology like strain gauges, piezoelectric transducers, capacitive transducers and optical sensors.

3.1.1 Strain Gauges

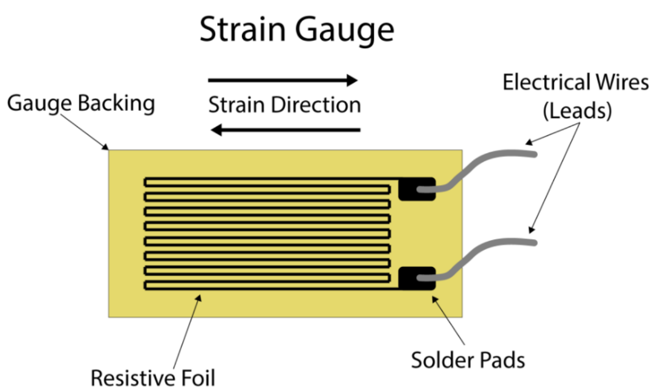

Figure 3.1: Strain Gauge [11]

Strain Gauges are a type of flexible sensor used to measure strain or deformation lengthwise. They are made up of a thin foil of conductive material placed on a zigzag pattern covered by a thin, insulating and flexible material. This creates a constant electrical resistance, as when a strain force is applied on the sensor, the foil deforms, changing its resistance. Due to their design features they are very susceptible to humidity and temperature changes [12]. For this reason they are commonly used in a Wheatstone Bridge configuration, generally composed of four strain gauges, although possible to only use two. [13].

3.1.2 Optical Sensors

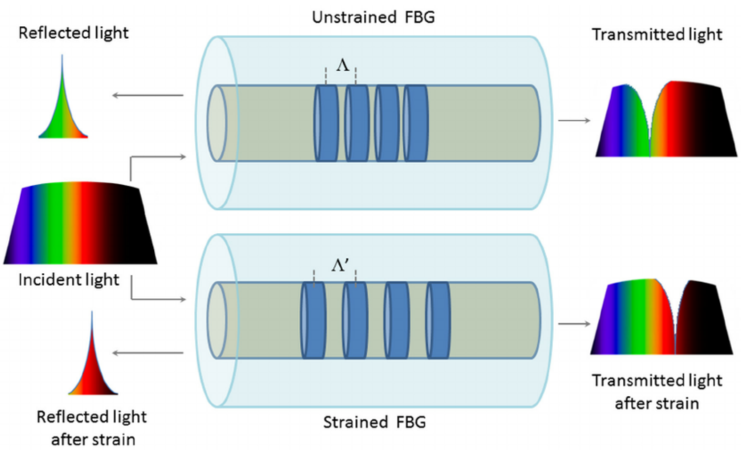

Figure 3.2: Principle of FBG [14]

An alternative sensor that holds some potential for implementation in this application is an Optical Sensor. One approach of Optical Sensors is composed of an emitter, a receiver and of some sort of Fiber Optics (FO) with a Fiber Bragg Grating (FBG). The FBG consists of evenly spaced reflectors on the core of the FO, which selectively affects a specific wavelength. They operate on the principle that when a Fiber Optics experiences a strain force, it undergoes slight stretching. This stretching alters the spacing between the reflectors in the FBG, resulting in a change in the wavelength that is reflected by the FBG (Figure 3.2). Due to being extremely sensible, this solution also enables measurements of temperature, pressure, flow and vibration and is already implemented for medical purposes such as monitoring of blood pressure or stroke volume [14]. Its most notable advantages are small size, great flexibility and also being immune to electromagnetic interference.

Another implementation mentioned in [14] is an Intensity Modulated Fiber Optics Sensor. In this case, it involves a Fiber Optics that varies the intensity of light passing through it based on the applied stress. Three different examples of this principle are depicted in Figure 3.3. They can use two Fiber Optics (**A**), a single Fiber Optics and a mirror (**B**) or a single FO that is bent (**C**). The distance, pressure or displacement can be measured based on the intensity of the light at the output.

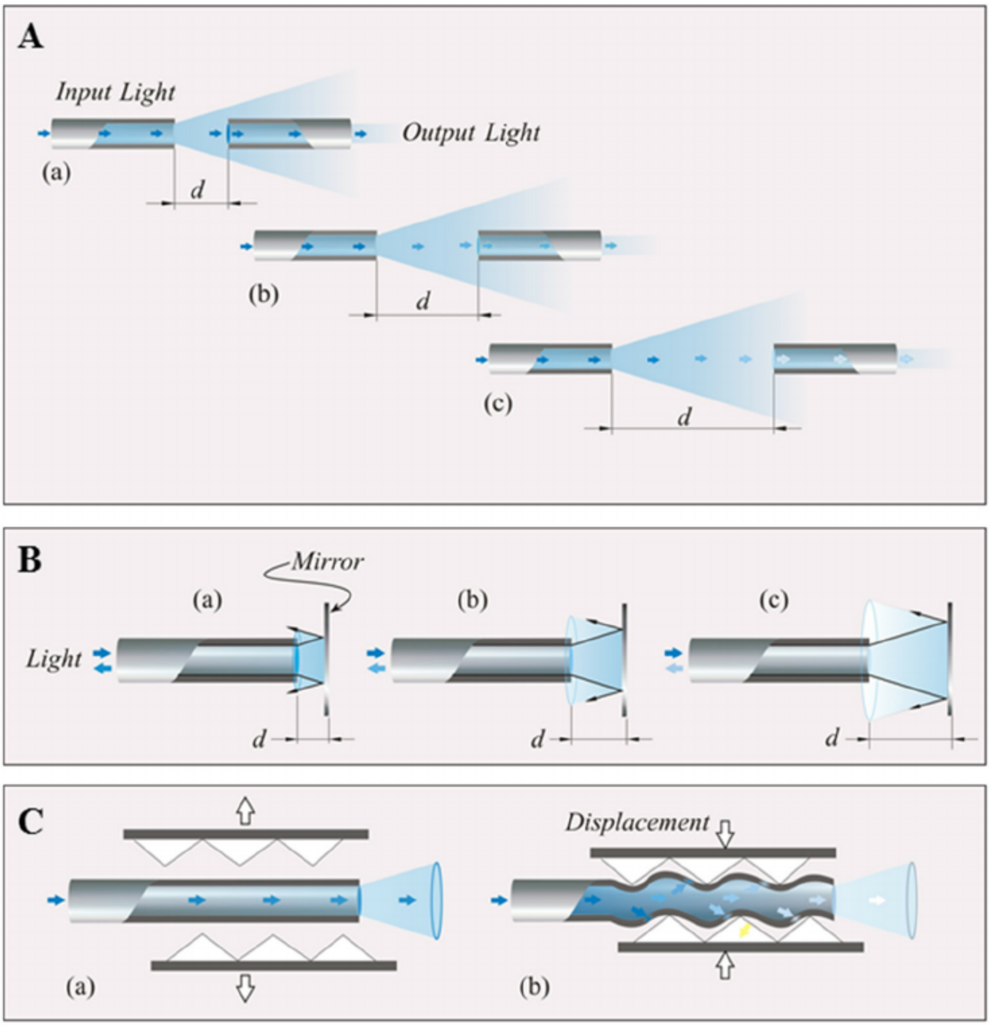

Figure 3.3: Principle of Intensity Modulated FOS [14]

3.1.3 Load Cells

The term Load Cell encompasses a range of force transducers, a type of sensor that alters an electrical signal proportionally to the force it is subjected to. One such transducer is the **Strain Gauge** 3.1.1 that when in a Wheatstone configuration is classified as Load Cell.

Other prevalent types are **Pneumatic** and **Hydraulic** Load Cells, very similar in principle. Both utilize a flexible diaphragm placed in a chamber with a Strain Gauge. Such diaphragm, when compressed, increases pneumatic or hydraulic pressure respectively, translating in an increase of force in the Strain Gauge.[15]

Some less common but relevant alternatives are **Inductive**, **Capacitive** and **Magnetostrictive** Load Cells.

3.1.4 Force-Sensing Resistors

Force-Sensing Resistors, also referred to as Force-Sensitive Resistors or FSR for short are sensors whose resistance changes when a force, pressure or mechanical stress is applied to them. They are made using multiple thin and flexible layers of conductive and non conductive material and as pressure is applied the resistance lowers. Once the pressure is released the resistance returns to the initial value. There are two types of FSR based on different types of construction Figure 3.4.

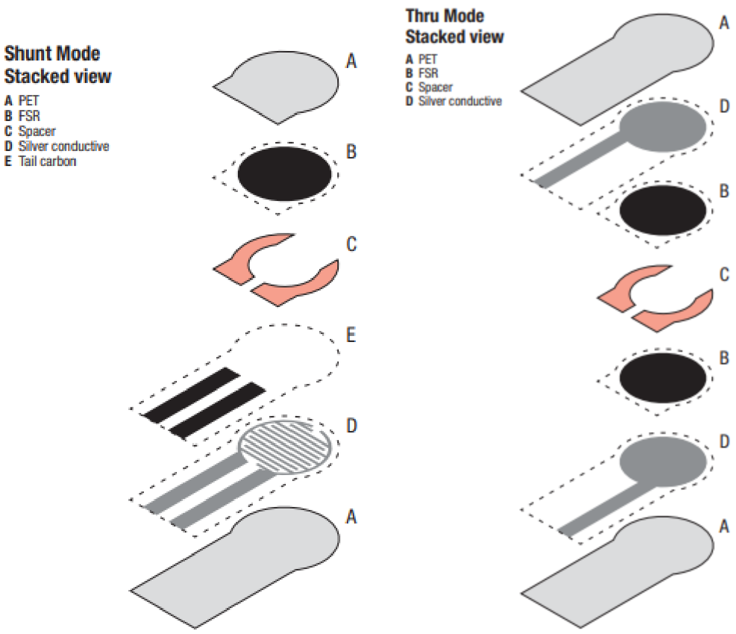

Figure 3.4: Shunt mode FSR and Thru mode FSR [16]

Shunt mode FSRs have a conductive layer arranged in an interdigitated finger pattern, while **Thru mode** FSRs utilize two solid conductive layers separated by a spacer. **Shunt mode** are simpler, more common, less expensive and work on a wide range of forces. On the other hand, **Thru mode** FSR are more complex and costly but they are more sensitive to weaker forces and their output is slightly more linear.

The problem with both types of sensors is that they are not absolute force sensors, more precisely, it is possible to calculate their resistance when subject to a given force but not quantify the force. Some manufacturers of FSRs provide the correlation between the resistance and the force that the FSR is subject to. Nevertheless, it is important to understand their accuracy. Taking into consideration that the force on the sensors can be unevenly distributed, that after repeated use the resistance is bound to deviate from the values of the datasheet when subjected to the same force, and that two equal sensors can have slightly different resistances, around 10% to 20%, it is possible to conclude that there is a certain amount of imprecision associated with the use of FSR, with some manufacturers going as far as informing that the sensors are better suited for qualitative information of the pressure rather than quantitative. That is the case for Adapttech®. It is necessary to obtain the relation between pressure in different parts of the socket but not its absolute value.

Despite the challenges and considerations mentioned earlier, the use of **Shunt mode** FSRs in the Adapttech® system is a suitable choice. **Shunt mode** FSRs offer several advantages that align with the requirements of the system. Firstly, they are widely available, making them easily accessible for integration. Secondly, they are relatively easy to manufacture, allowing for cost-effective production. Additionally, their thin and flexible nature is crucial for minimizing their impact on the socket fitting, ensuring a comfortable and optimal fit for the user. Taking in consideration the desired use for such sensors, it is not crucial that they tell us the precise pressure on a given part of the socket, but rather the points with relatively higher and lower pressures, which should be coherent with design constraints of the prosthetic socket and the location of pressure-tolerant and pressure-sensitive areas of the residual limb.

Moreover, it is crucial to understand the role that air has in Force-Sensing Resistors. The conductive terminals are separated by a resistive layer. The working principle of the above-mentioned sensors is that as the pressure they are subject to increases, the surface area of contact between the resistive layer and the terminals also increases, and, as such, the resistance between terminals lowers. After the pressure is released, the sensor returns to its initial state where the terminals are separated, resembling an open circuit. This separation is ensured by the spacer in the sensor construction. When the flexible layers of the sensor are separated to their original state, it creates a space where air is introduced between the conductive and resistive layers. This air acts as an insulator, preventing direct contact between the layers. The opposite occurs when pressure is applied and the air is forced outwards in order to reduce the resistance. The air is expelled and absorbed through an air vent, visible in Figure 3.4 ,enclosed by the terminals. The presence of an air vent is a standard feature in most FSRs and crucial for ensuring precise measurements. When the air vent of the sensor is obstructed or restricted, the air trapped between the layers offers resistance to the pressure applied. This resistance reduces the surface area of contact between the layers, leading to inaccurate measurements. It is important to ensure proper ventilation of the sensor to maintain reliable and accurate pressure readings.

FSR technology is vastly used in similar areas, for example the aforementioned F-scan and F-socket by Tekscan. 2.2.2

3.1.5 Piezoelectric Sensors

Piezoelectric Sensors are a type of sensor that operates based on the piezoelectric effect, derived from the Greek word *πιέζω* (*piézō*) meaning "to press". The piezoelectric effect refers to the generation of a measurable surface charge across certain crystalline materials when subjected to mechanical force. This charge can be expressed into voltage via the relation $Q = CV$ where Q represents the stored charge measured in Coulombs, C the capacitance in Farads, and V the voltage in Volts. The polarization occurs due to the alteration of the relative positions of positive and negative charges, resulting in a net polarization [17, 18]. The types of materials that most commonly exhibit piezoelectricity are:

- Natural piezoelectric materials: for instance quartz (crystalline SiO_2)

- Polycrystalline ceramic materials subjected to poling: for instance barium titanate ($BaTiO_3$)
- Polymers: for instance polyvinylidene fluoride (PVDF)

Poling is a process in which the material is heated above the Curie temperature (conferring high mobility to the dipoles) and a strong electric field is applied. Piezoelectric materials can be used to manufacture mainly two different types of sensors, force sensors and accelerometers.

3.1.5.1 Piezoelectric force sensors

Focusing on piezoelectric force sensors, they are primarily employed to measure applied force, but also pressure or strain. Unlike other traditional force sensors that rely on elastic elements, piezoelectric sensors do not require elastic components. This characteristic results in reduced loading errors because the deformation of the sensor is negligible in most cases. Furthermore, the relation between force and the resulting voltage is highly linear, even up to thousands of volts [17, 18].

However, these sensors are characterized by some disadvantages. They exhibit high temperature sensibility, and their surface charges are particularly susceptible to neutralization by environmental charges, dielectric current leakage, and most importantly input resistance of the interfacing electronics. As a result, these sensors behave as a high-pass filter for input signal, which makes static measurements challenging. They are more commonly employed to detected rapid changes in force, pressure or strain [17].

3.2 Calibration

Calibration is crucial to ensure accurate and precise measurements, the foundation for quality and safety [19]. Without calibrated instruments, it is not possible to achieve consistency and reliability, which can result in uncontrollable risks, increase in costs or even the loss of market confidence, in specific applications [20]. Calibration is indispensable across various fields and for different types of sensors. Two calibration methods for Force-Sensing Resistors are comprehensively examined and discussed.

3.2.1 Creep and Hysteresis compensation

To improve the reliability of FSR data, it is recommended to subject them to a calibration process. A basic way of implementing this is simply applying constant and know forces (for example placing different weights on top of them) and obtaining the relationship between the resistance and force, to compensate for the non-linear specific response of a particular FSR device.

As shown by J. A. Flórez and A. Velásquez in [21], one can understand that, when using FSRs, two undesired effects occur. The first effect is known as creep, which refers to the tendency of the FSRs resistance to slightly decrease over time, eventually stabilizing when subjected to a constant force. Creep can lead to inaccurate measurements if not accounted for. It can create the impression of an increase in pressure or force, which may misrepresent the actual conditions. Another undesired effect observed in FSRs is hysteresis, which occurs when the sensor's output is influenced by the previous history of the system. In the case of dynamic loads, hysteresis can affect the resistance values of the FSRs. Specifically, the resistance for a given force may differ depending on whether the previous force applied to the sensors was greater or lower. The article additionally discusses two compensation methods: one for addressing the creep effect, which involves considering the derivative of the voltage with respect to time, and another for handling hysteresis, which employs a more sophisticated approach utilizing a fourth-degree polynomial.

The impact of both effects needs to be thoroughly studied for the case use of Adapttech® system. However it is expected that hysteresis will have a greater impact than the creep effect since the system is commonly used to evaluate the pressure distribution when performing dynamic tasks such as walking. The article goes on to recommend avoiding simultaneous correction of both negative effects due to potential performance degradation. Only after conducting extensive tests and confirming the findings, hysteresis compensation might be considered as a suitable solution.

3.2.2 Adapttech® Calibration Method

As discussed previously in subsection 3.1.4 there is an imprecision associated with FSRs. For that reason Adapttech®'s team performed tests to evaluate this imprecision. Two different tests were performed, one using a reference circuit and the other using INSIGHT™'s sensors custom Processing Circuit. Using data collected in these tests, the inter-sensor variability was estimated at around 20-25% in the voltage response. Having a inter-sensor variability of 20-25% meant that, in order to obtain precise pressure data, each FSR sensor of the strip needs to be calibrated individually as opposed to simpler approaches considering the average output.

After literature review, the team also concluded that the pressure range of interest inside the socket was between 0-3.5 *bar*. This pressure range is much narrower than the dynamic range of the FSRs present on the strips. In order to better guarantee a linear behavior this must also be addressed in the calibration.

Using INSIGHT™ sensors custom Processing Circuit without implementing any calibration method a logarithmic relationship between the voltage and the pressure applied on the sensor is obtained, as expected.

For calibrating the system, a pressure cycle was idealized. This pressure cycle varies from 0 to 3.8 bar stopping at predefined pressure steps where FSR data will be acquired. This pressure cycle has three different modes:

- **Intake**: The pressure starts in 0 bar and progressively increases to 3.8 bar;
- **Outtake**: The pressure starts in 3.8 bar and progressively decreases to 0 bar;
- **Intake and Outtake**: The pressure starts at 0 bar and progressively increases to 3.8 bar, afterwards the pressure progressively decreases back to 0 bar.

They are used for testing and calibrating, the **Intake and Outtake** method being the one that produces the most accurate results.

The linearization of the output is obtained with equation 3.1, where ADC_{New} is the new 0-255 value, whereas ADC_{Old} is the old 0-255 value obtained by the ADC, and there are also two sensor specific parameters, m for slope and b for y axis bias:

$$ADC_{New} = e^{\frac{ADC_{Old} - b}{m}} \tag{3.1}$$

An INSIGHT™ 8 sensor strip will, therefore, have 16 calibration parameters. These are the values the calibration procedure estimates, by comparing sensor response (while known and relevant pressure values are being applied) with an ideal linear response in the range of interest.

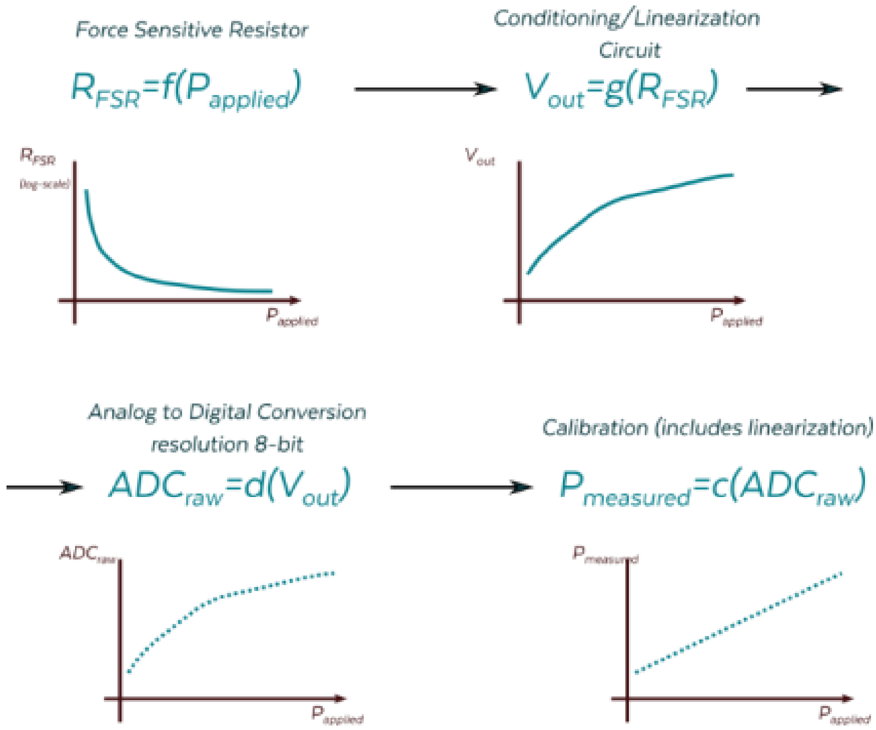

Figure 3.5: Evolution of Sensor Output

Figure 3.5 displays an overview of the evolution of the applied pressure until the linearized measurement of pressure. $P_{applied}$ stands for the pressure applied on a given FSR cell, R_{FSR} for the resistance of the FSR cell, V_{out} represents the voltage after the conditioning circuit, ADC_{raw} the voltage sampled by the ADC and $P_{measured}$ the linearized pressure for that FSR cell.

3.2.2.1 Curve Fitting

As mention previously, the FSR's dynamic range is greater than the pressure range of interest. As a consequence of this, and with the goal of increasing the accuracy of the system, the calibration procedure must normalize the scale, ensuring that the ADC maximum is achieved at around 3.5 *bar*.

Another important consideration is that the response to the absence of pressure on the sensor is *6*, this bias is introduced by the signal Processing Circuit. This will be useful later to detect faulty or unresponsive sensors but also needs to be considered on the ideal response. Therefore, the ideal linear response given the relevant range can be obtained by equation 3.2.

$$ADC_{New} = Pressure_{bar} \times \frac{255-6}{3.5} + 6 \tag{3.2}$$

This equation translates into the plot of Figure 3.6, where the blue line represents the ideal linear response and in orange are the upper bound of 255 and the lower bound of 6.

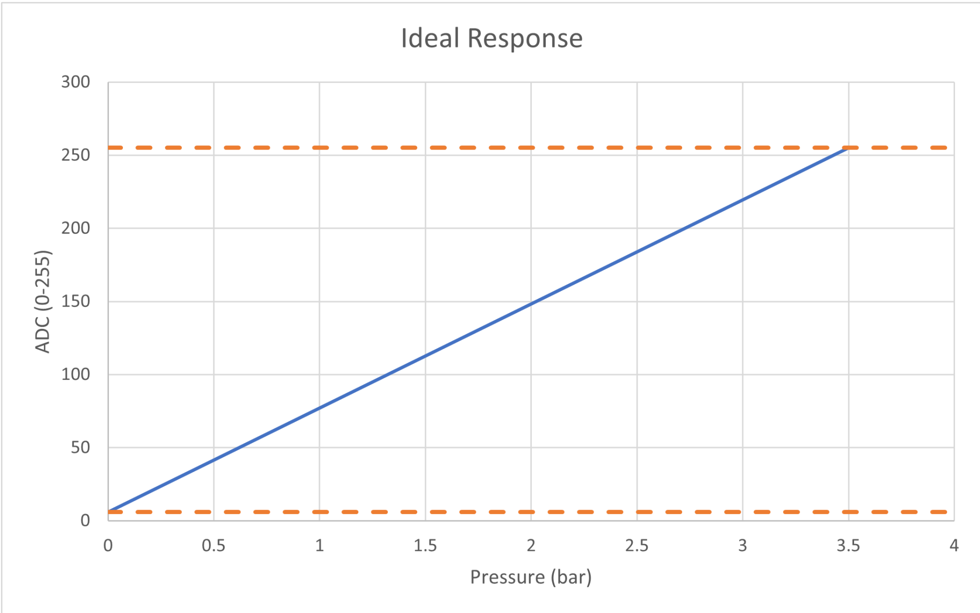

Figure 3.6: Ideal Linear ADC response

To obtain *m* and *b* parameters, a curve fitting method is used. This method consists of finding an optimal set of parameters to better fit a set of data to a defined function. In this case, curve fitting, finds *m* and *b*, parameters of a linear regression that best fit the response of a given sensor to the ideal response (equation 3.2).

Using the equation 3.1 with the parameters obtained with the curve fitting method, the FSR's response is approximated to a linear ideal response.

3.2.2.2 Criteria for accepting calibration parameters

The calibration method does not produce an expected range of calibration parameters *m* and *b*. To ensure that erroneous calibration parameters are detected one must consider the response range as a two dimensional space.

There are three requirements that are applicable for all the sensors. These requirements are as follows:

- The raw sensor response at 3.5 bar must be at the minimum 120 and at the maximum 255;
- The raw sensor response at 0.5 bar must be at the minimum 20;
- The raw sensor response at 0 bar must be at the maximum 10.

With these requirements, a 2D solution space can be obtained as shown in Figure 3.7.

To test a set of calibration parameters, simply trace them in this two dimensional space and if they are in the solution space (green area marked with 1) it is possible assume they are valid. All the other parameters that are not inside the solution space are marked as invalid and the entire strip is discarded.

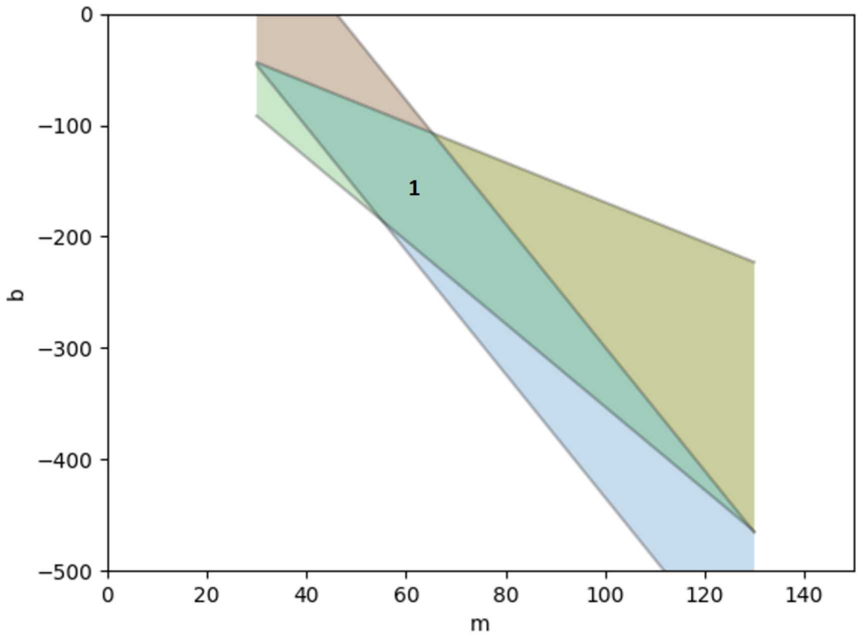

Figure 3.7: Two dimensional solution space. In green (marked by 1) is the acceptable combination of *m* and *b*

3.3 Conclusion

Numerous sensors where presented with possible application for our system. It is important to understand how they compare with each other. Table 3.1 compares different sensors across several categories.

Regarding calibration methods, the method used in the Pressure Sensor Automatic Calibration System was the one already implemented, referred in Chapter 3.2.2, as this calibration method

Table 3.1: Comparison of different sensor technologies

Sensor Technology	Advantages	Disadvantages	Output
Strain Gauge	Reliable, accurate and versatile	Susceptible to humidity and temperature	Resistance
Optical Sensors	Small size, flexible and immune to electromagnetic interference	Very sensible to temperature changes and strain, without the ability to distinguish the cause	Wavelength shift or Light Intensity
Force-Sensing Resistors	Lightweight, thin, flexible, inexpensive	Substantial sensor to sensor difference, logarithmic output, require an air vent	Resistance
Piezoelectric Sensors	Thin, flexible, no moving parts	Better suited for dynamic applications, complex circuitry	Voltage

was already thoroughly tested and validated. It is, however, crucial to understand this method to ensure a correct implementation.

Chapter 4

INSIGHT™ Sensors and Manual Calibration System

This chapter discusses the INSIGHT™ Sensors and previously implemented manual calibration system developed by Adapttech®'s team.

4.1 INSIGHT™ Sensors

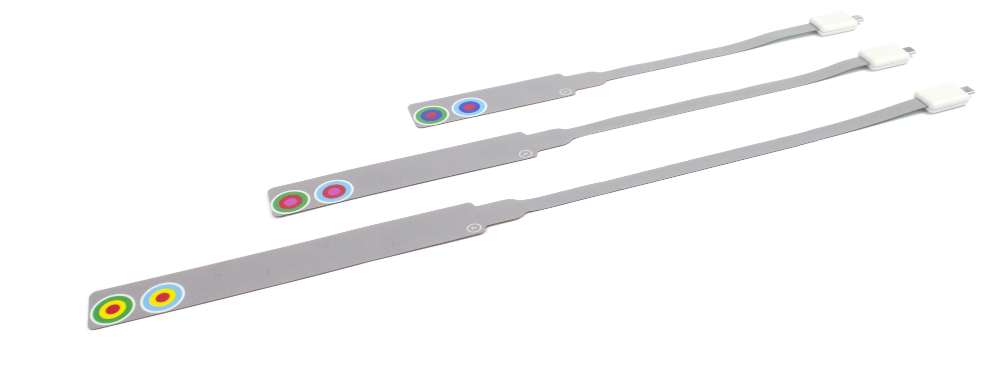

Figure 4.1: INSIGHT™ Sensors

Responsible for evaluating the pressure distribution inside the socket, INSIGHT™ Sensors are available in 3 different sizes (Figure 4.1), making use of Force-Sensitive Resistors, as aforementioned. The sizes are small, medium and large using 4, 6 or 8 FSR sensors respectively. The strips, as INSIGHT™ Sensors are also referred to in this dissertation, have a sticky layer on the surface which should adhere, allowing them to be temporarily glued to the socket.

4.1.1 Circuity

Encapsulated in a white plastic shell, there is a PCB responsible for processing the FSRs output and communication with the Wearable through USB type C. The block diagram of the sensors can be seen in Figure 4.2.

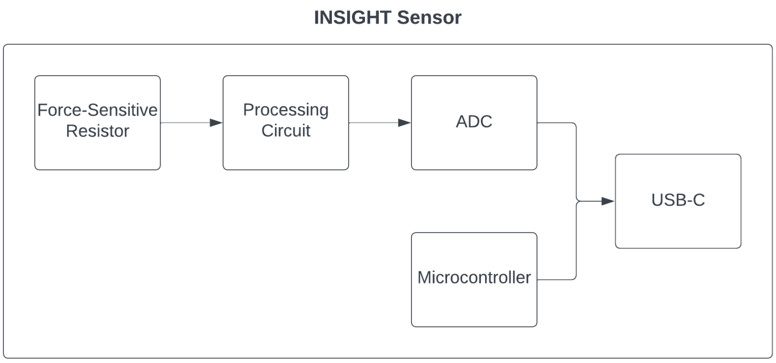

Figure 4.2: INSIGHT™ Sensors Block Diagram

Each strip contains a shared bus connected to all the sensors, which is linked to the ground, as well as individual buses dedicated to each FSR of the strip, connected to a signal Processing Circuit. The Processing Circuit is composed of an op-amp in a non-inverting configuration. There is one Processing Circuit per FSR and their outputs are connected to an 8 channel, 8 bit Analog-to-Digital Converter. The ADC converts the analog output of the op-amp to a value between 0 and 255 that is transferred to an external device via SPI protocol.

Furthermore, a dedicated AVR 8-bit microcontroller is responsible for performing essential tasks such as processing external requests and responses, enabling and disabling the strip LED, store strip data (calibration, ID, Manufacturer Part Number, etc.). This microcontroller is also connected to the external device via the USB interface.

4.1.2 Identification Number

Each strip possesses an ID printed at the bottom, which is crucial for correct system configuration. Moreover, this ID is translated into a color code allowing the INSIGHT™ Digitizer to not only locate the strip but also identify it, knowing in which location in the socket representation to display the applied pressure and animate the iOS app embedded graphics of pressure distribution.

The IDs range from 1-16 for small size strips, 17-32 for medium and 33-48 for large, meaning that the strip size can be extrapolated from the ID. This ID is not to be confused with the serial number of the strip which is unique to each strip. Instead, this ID repeats from system to system but must not be repeated in one given system.

4.1.3 Negative Aspects

Currently, the INSIGHT™ Sensors have some less positive aspects. The current response of the sensor does not utilize the entire range of the ADC, resulting in reduced precision for the system. As typical with FSRs there is also a need for an air vent that can interfere with the results if restricted.

Furthermore, in the specific use case of the INSIGHT™ system, it is crucial to minimize the interference of the strips in the fitting of the prosthesis while ensuring good adhesion to the socket. The bottom layer of the strip, responsible for attaching the strips to the socket needs to be thin, flexible and strong enough to prevent movement inside the socket. At the same time, it should allow for easy removal of the strips without leaving any residue. However, after a recommend number of uses, it is no longer guaranteed that the adhesive is capable of meeting these requirements.

Some of this aspects will be later address in chapter 6.

4.2 Manual Calibration System

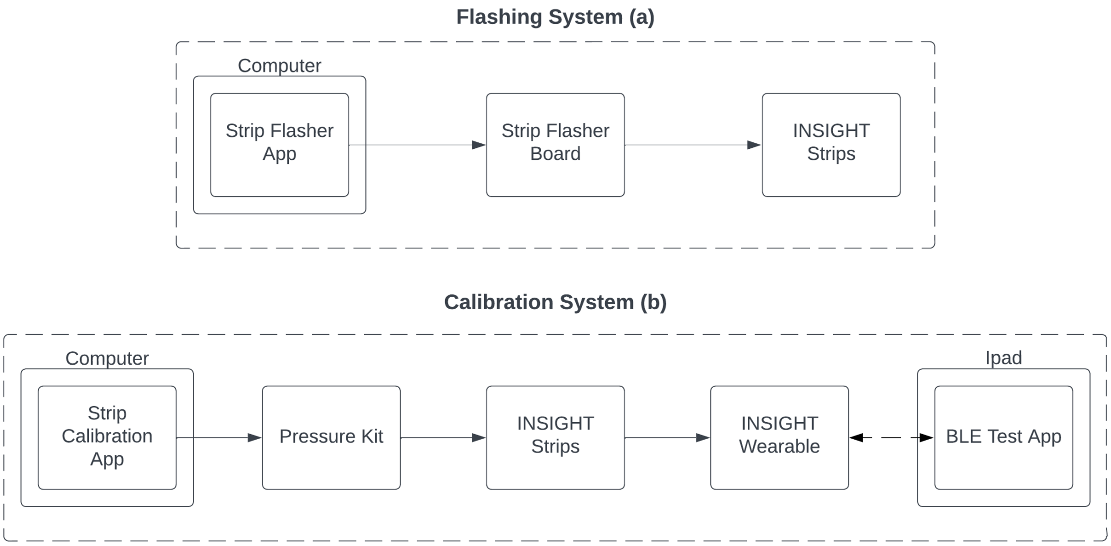

Figure 4.3: Block Diagram of Previous System

The manual calibration system is divided in two independent subsystems (Figure 4.3). The first subsystem **(a)** is responsible for flashing the firmware onto the INSIGHT™ Strips whilst the second **(b)** executes the calibration procedure.

4.2.1 Workflow

The Workflow of the manual calibration system can be seen in Figure 4.4 and Figure 4.5.

The calibration process begins with an operator inserting the desired strips, up to a maximum of 16, into the Strip Flasher Board. With the board connected to the computer, the strips are flashed using the Strip Flasher App.

After the flashing process is concluded, the operator must disconnect the strips from the Flasher Board, insert them inside the pneumatic press and connect them to the Wearable. Afterwards a Windows and a iOS application are run simultaneously. These applications are described with greater detail in Subsection 4.2.3.2 and Subsection 4.2.3.4, respectively. When the press reaches the desired pressure step, the operator must input the pressure read by the sensor, press update and then press snap. This is repeated for each pressure step.

Afterwards, the Wearable saves a file with the information collected. This file is then processed by another separate application that generates the calibration parameters. Finally said parameters are uploaded to the device's *EEPROM* by the Wearable.

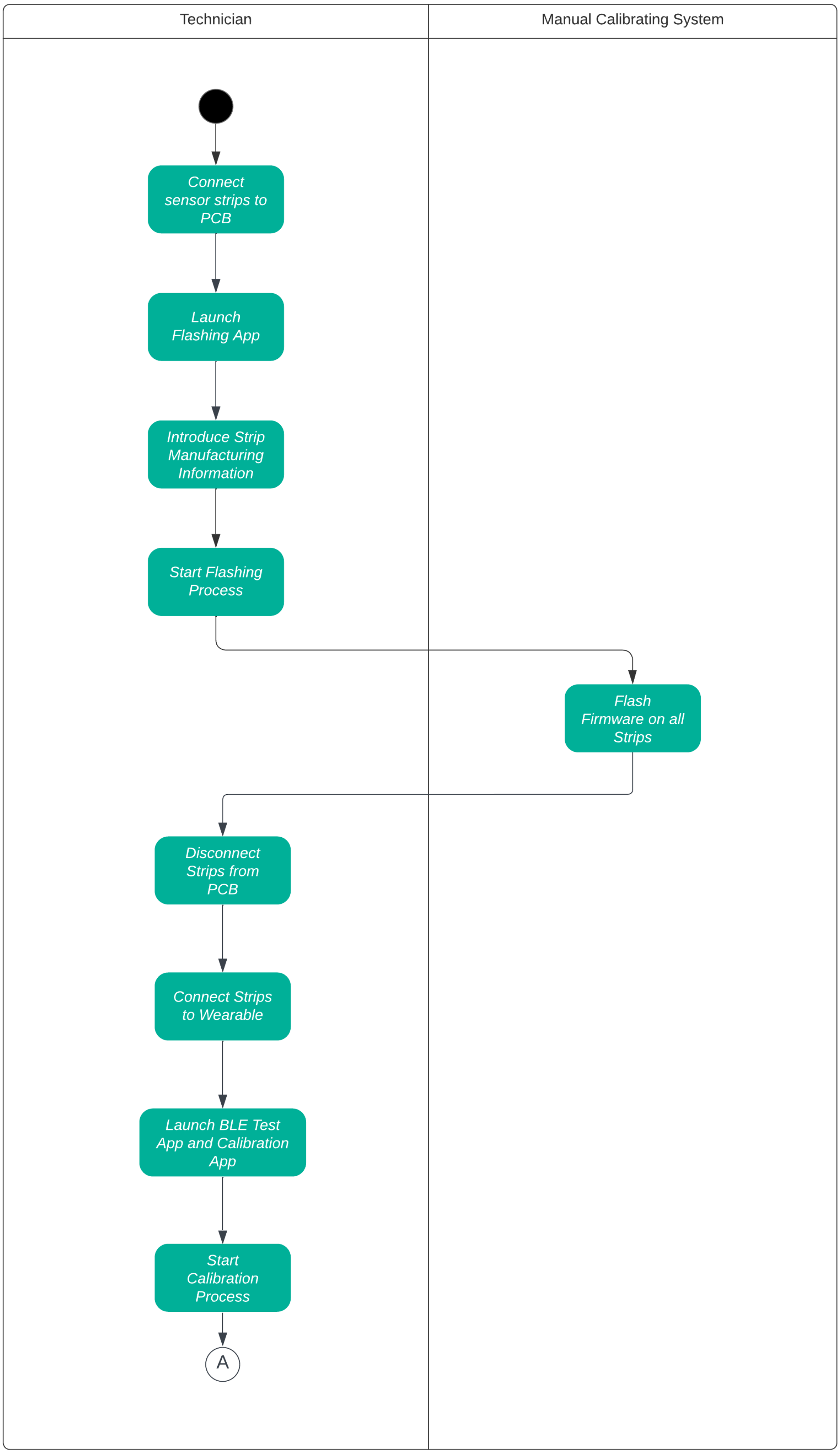

Figure 4.4: Activity Diagram of Manual System (part 1)

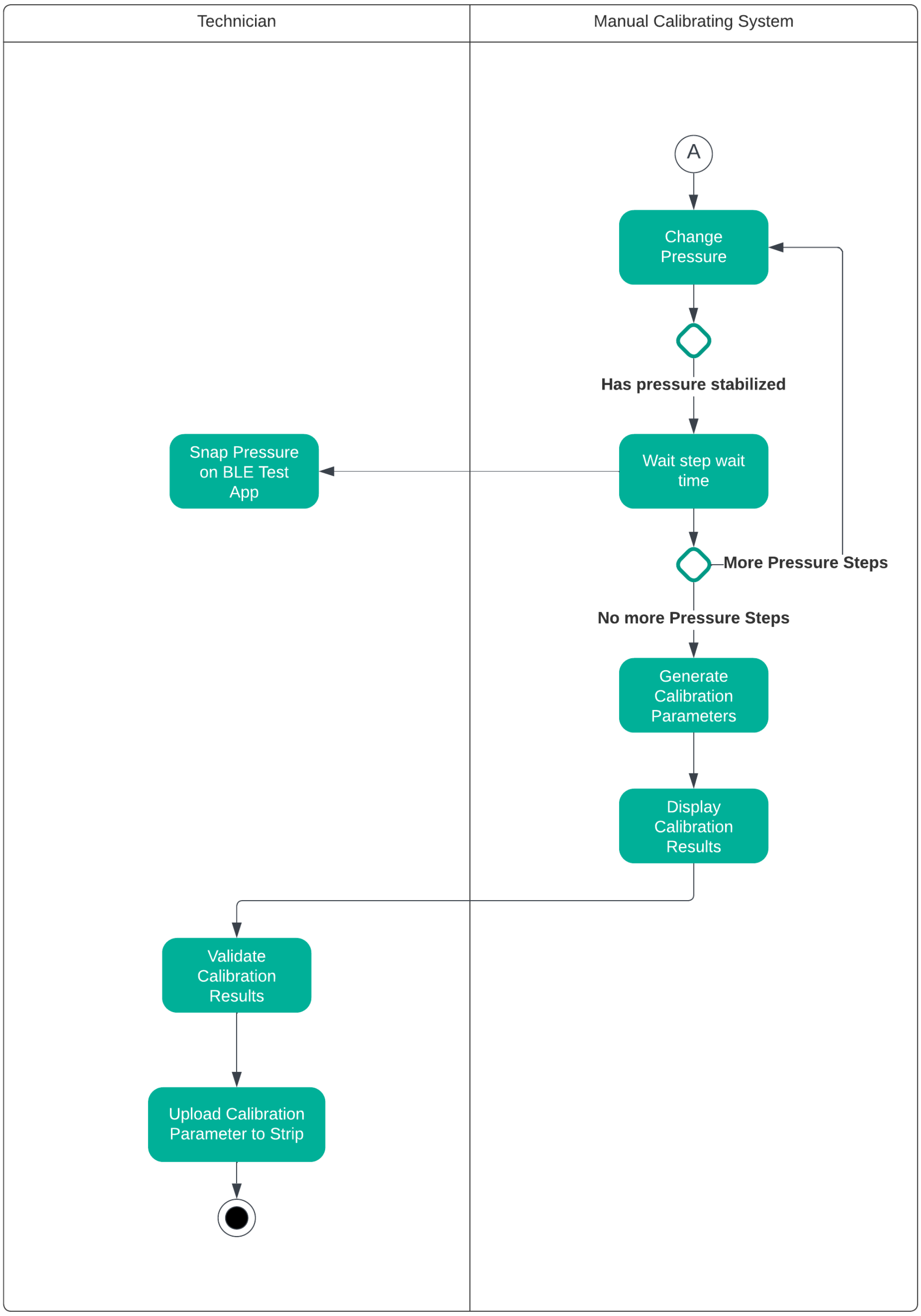

Figure 4.5: Activity Diagram of Manual System (part 2)

4.2.2 Flashing System

The flashing subsystem is composed of a computer running the Strip Flasher App, a Strip Flasher Board and the INSIGHT™ Strips.

4.2.2.1 Strip Flasher App

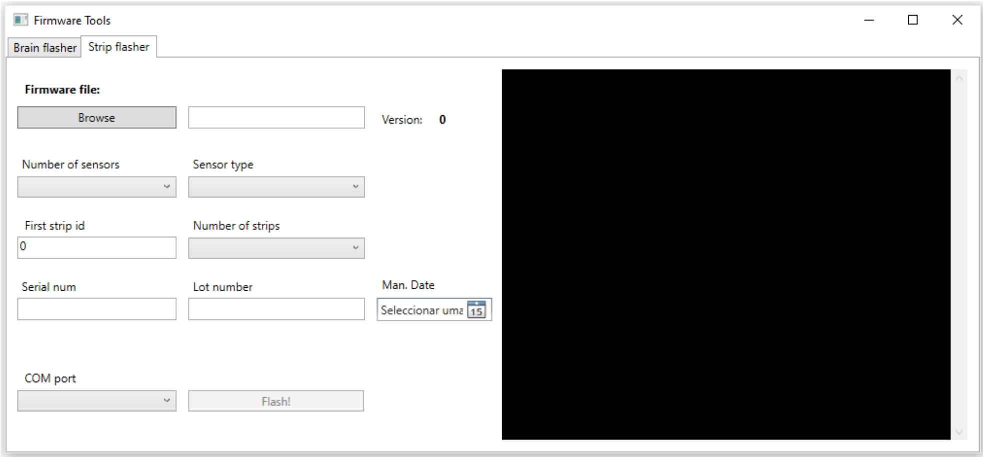

Figure 4.6: Strip Flasher App

The Strip Flasher App (Figure 4.6) developed by Adapttech® is a Windows application responsible for flashing the strips with the latest firmware and write, in the strip's *EEPROM*, data regarding the serial number, the strip size (4, 6 or 8 sensors), the Lot number, the strip ID (depending on the strip size and it can go from 1 to 48) and the manufacturing date. Once the relevant data is selected, the app flashes the strips utilizing the AvrDude utility. AvrDude is a program used to manipulate the *ROM* and *EEPROM* contents of AVR microcontrollers using the in-system programming technique (ISP).

4.2.2.2 Strip Flasher Board

The Strip Flasher Board is a PCB designed to establish the communication between the computer and the Strips. The strips the program want to communicate with must be specified by sending a command from the computer, This command is interpreted by the microcontroller and the correct strip is selected using multiplexers.

As shown in Figure 4.7, there are 8 slots available for strip connection. However, stacking a master PCB on top of a slave, expands the number of slots to 16. In virtue of the way this PCB was designed, a slave Strip Flasher Board is identical to a master, with the exception of having no electronic components and having female header pins as opposed to male.

The slave PCB connects to the master using the header pins represented by the yellow block (nr. 1). The red block (nr. 2) indicates communication components, lika a serial to USB converter, and allows the connection between the microcontroller and the computer. The microcontroller

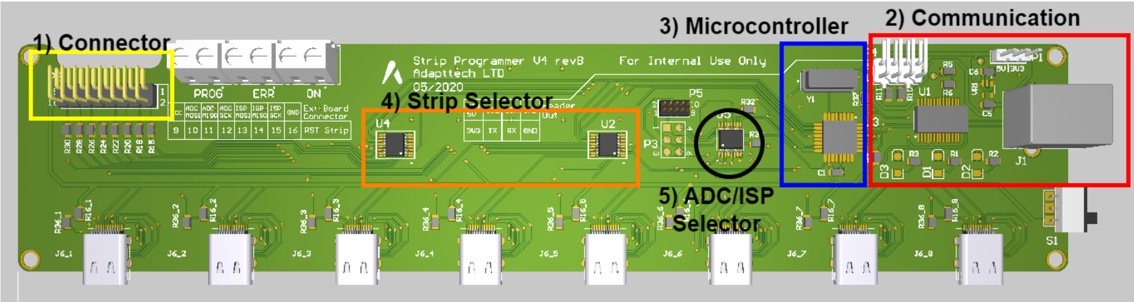

Figure 4.7: Front view of Strip Flasher Board (length: 220mm)

(ATMEGA328) and his external crystal are highlighted by the blue rectangle (nr. 3) . It is responsible to parse the commands sent by the PC and process them.

The strips are connected to the PCB via USB Type C. The orange block (nr. 4) represents the strips selector. It is composed by two multiplexers, one for the “master” slots, another for “slave” slots. There is also another multiplexer, in the black circle (nr. 5), to choose between *ADC SPI* and *ISP SPI*. This allows to chose if the board is going to flash the strips or use the *ADC* to obtain the data from the strips sensors. However this feature was previously bypassed by a set of 3 jumpers only allowing the board to flash the strips Figure 4.8 (nr. 6).

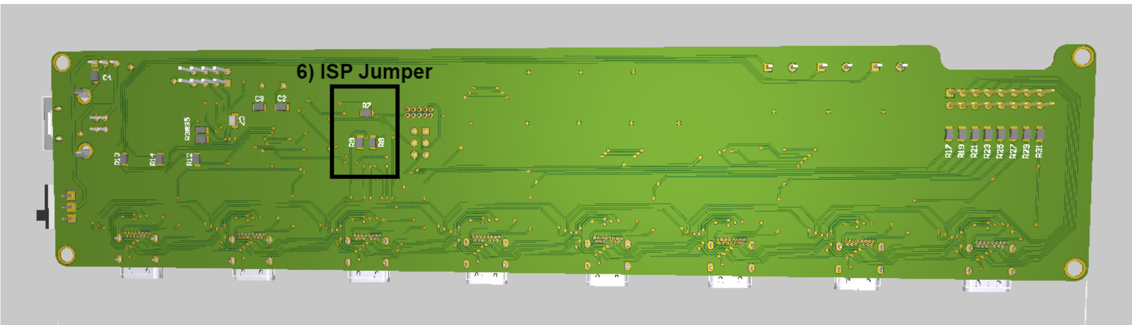

Figure 4.8: Back view of Strip Flasher Board

4.2.3 Calibration System

The calibration subsystem (Figure 4.9) is composed of a computer running the Strip Calibration App, the Pressure Kit, INSIGHT™ Strips, INSIGHT™ Wearable and an iPad running the BLE Test App (see Figure 4.12).

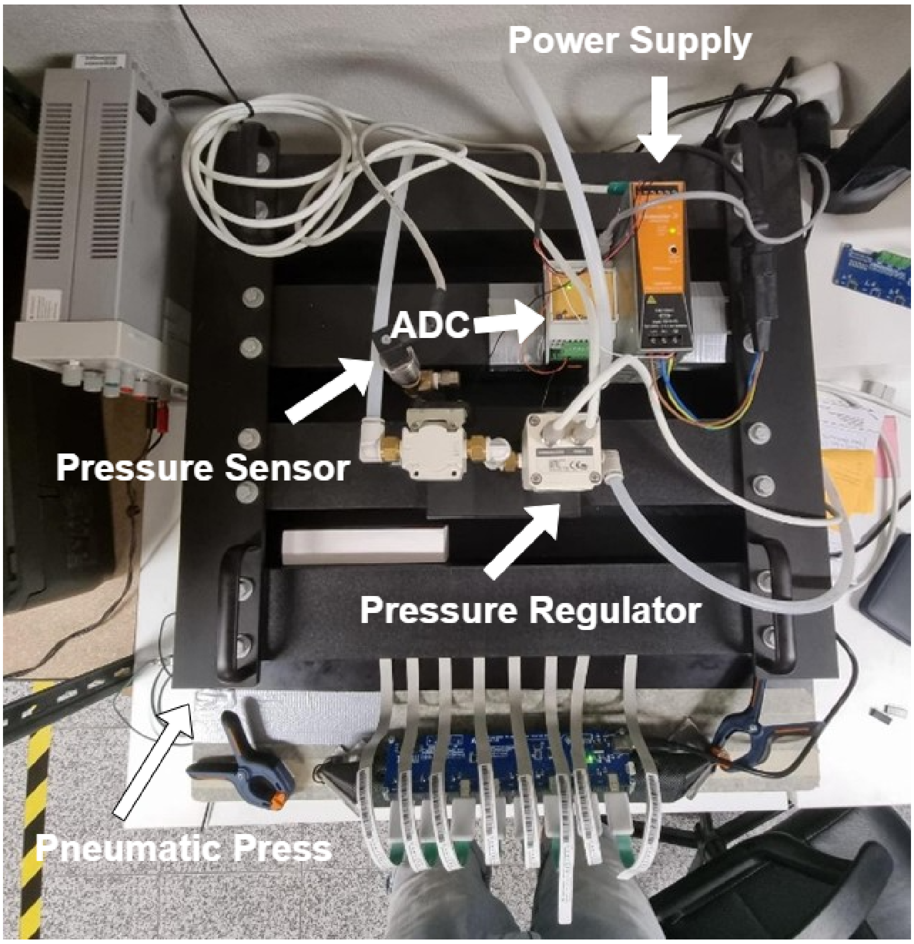

Figure 4.9: Top view of previous calibration system

The computer ensures the Pressure Kit executes a pressure cycle stopping at predetermined pressure steps. Using the Wearable and BLE Test App the operator collects data from the strips.

4.2.3.1 Pressure Kit

The Pressure Kit is a precision pressure control system that contains four main parts:

- **Pneumatic Press and Air Compressor**: These devices work together to apply even pressure on the sensor strips.
- **Pressure Regulator**: The Pressure Regulator, a **SMC RS-232C** model, communicates with the computer and sets the target pressure. It is connected to the Air Compressor and the Pneumatic Press. By controlling the airflow, it increases or decreases the pressure applied to the strips.
- **Pressure Sensor**: The system utilizes a pressure sensor, the **RsPro 797-5037** model, to accurately measure the exerted pressure within a range of 0 to 10 bar, with a precision of $\pm 0.25\%$. To interface with the computer, a **LucidControlAI4** ADC is employed.

- **Power Supply**: The power supply used in the system is a **Weidmuller Pro Eco (120W 24V 5A)**. It provides power to the Pressure Regulator, Pressure Sensor and ADC.

4.2.3.2 Strip Calibration App

To handle the calibration system, a C# based application is used (Figure 4.10). It is a web application with a GUI and it is responsible for managing all the communications and cycling through a set of pressure values defined by the user. The application is not optimized to work with the Strip Flasher Board and, for this reason, it can not collect data from the sensors to perform the calibration. Instead the operator must use the INSIGHT™ Wearable and BLE Test App

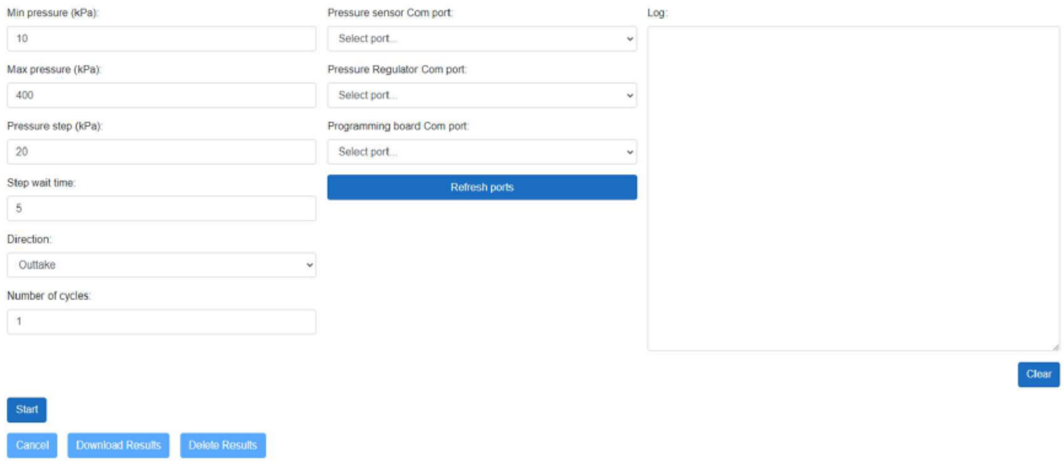

Figure 4.10: Strip Calibration App

The Strip Calibration App allows the operator to select the parameters for the pressure cycle like minimum pressure, maximum pressure and pressure step or step wait time which is the time in seconds that the system remains at a given pressure value before advancing to the next pressure step (its relevance is explained later). Additionally it is also possible to configure the number of pressure cycles and the COM Ports of the Pressure Regulator, and Pressure Sensor. The COM Port of the Strip Flasher Board may also be selected, despite being irrelevant as this feature was never implemented.

4.2.3.3 INSIGHT™ Wearable

Figure 4.11: INSIGHT™ Wearable (length: 20-45cm depending on version)

The INSIGHT™ Wearable (Figure 4.11) is connected to the strips via USB-C. It is used in the calibration process for reading the strips ADC, working collectively with the BLE Test App. After the calibration is completed and the calibration parameters are generated, the Wearable is responsible for uploading said parameters to the device *EEPROM*.

4.2.3.4 BLE Test App

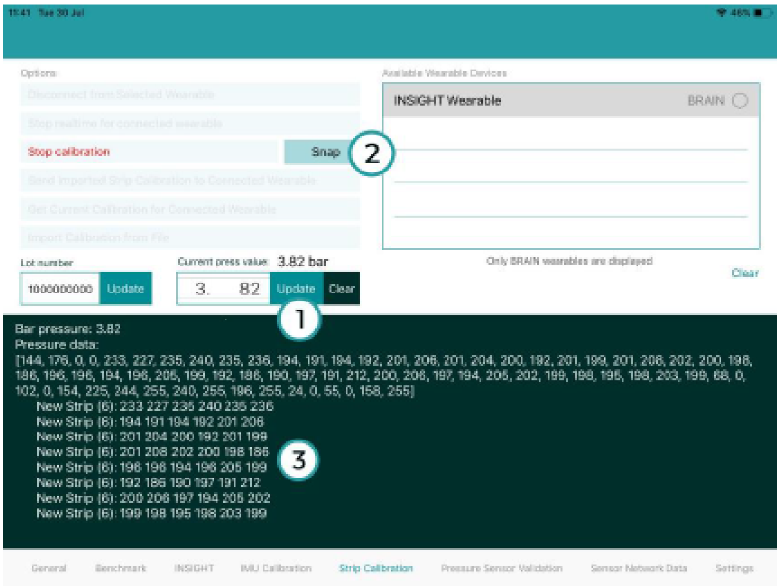

Figure 4.12: INSIGHT™ BLE Test App

The BLE Test App (Figure 4.12) is an iOS application developed by Adapttech®'s Software team used in several development and testing operations like the calibration process. In the calibration process, as the pneumatic press reaches each desired pressure step, the operator manually inputs the pressure read by the sensor into the Strip Calibration App, presses the "update" button (**1**), and then clicks the "snap" button (**2**). The collected pressure data is shown in (**3**). This process is repeated for each pressure step.

4.2.4 Negative aspects and improvements

The previous system is able to provide a accurate calibration however it requires high human intervention and constant attention from an operator. At the same time, it also requires to switch between different applications and connect the sensors to multiple interfaces. Having a system with considerable human factor, increases the probability of errors occurring.

One critical step of this process is the selection of a correct step wait time. If insufficient, the app may take the snapshot when the press has already started to shift to the next pressure step. All sort of distractions may also affect when the operator presses the snap button on the BLE Test App. This will lead to a decrease in the quality and accuracy of the calibration.

Furthermore, the operator has to have an overview of the output of the calibration process of each sensor. If the operator is calibrating sixteen strips of eight sensors each this means that the operator must overview one hundred and twenty-eight calibrations.

The proposed automatic calibration system includes all these processes in a single application, only requiring an operator to setup the system and initialize it. The system then proceeds to autonomously flash the strips, run the calibration cycle while collecting data, process that data to obtain the calibration parameters and detect errors in the sensors. Finally it writes the calibration parameters on the strip *EEPROM*.

Minimizing the human factor and time sensitivity of the process increases the reliability, quality and accuracy of the process resulting in a reduced probability of error.

Additionally the proposed automatic system gives the possibility of being implemented as a stand alone system using a embedded single board computer like a Raspberry Pi.

Chapter 5

Automatic Calibration System

In the previous chapter, it was discussed that the current calibration system is characterized by its complexity, slow operation, allowance for error and the need for continuous operator supervision. In light of these challenges, an automated system has been developed, taking into consideration the available equipment and materials within the company, with the aim of reducing costs and production time.

The new calibration system was developed using the Python programming language. This decision was made considering that Python provides a straightforward approach for communication, file manipulation, creating a GUI and also is supported by multiple platforms, if later desired may be effortlessly implemented on a Raspberry Pi.

With the implementation of this new system, it is anticipated that the operator will only be required to perform the initial setup, while the subsequent steps will be carried out autonomously. As a result, the time spent by the operator is expected to be reduced to less than three minutes.

5.1 System Requirements

After familiarization with the Manual Calibration System and studying the necessary improvements, the system's requirements for the new automatic calibration system were defined.

- Functional Requirements:
  - The system must be able to flash the strips with the latest firmware version;
  - The system must perform a calibration, based on the manual system;
  - The system must allow testing of different sensors;
  - The system must detect connection errors;
  - The calibration parameters must be approved or rejected by the system based on determined criteria.

- Non-Functional Requirements:
  - The system must have a user friendly interface.
- Performance Requirements:
  - The system must minimize the amount of time that an operator is needed;
  - The system must produce calibrations as accurate as the previous system;
  - Ideally the process should be faster than the previous system.
- Constraints:
  - The system must use the equipment and material already available at the company.

Considering the system requirements, the system was conceptualized to have a computer executing a Windows application. This application serves as the central control hub, responsible for managing the pressure system, establishing communication with both the pneumatic press and the pressure sensor. Furthermore, the application is designed to establish a seamless connection with the Strip Flasher Board, which serves as the interface for connecting the sensor strips. The main functions of the application would be to execute pressure cycles while collecting data from the sensors, generate calibration parameters for the valid sensors, and flash the strips with the latest firmware and correct calibration parameters. Figure 5.1 shows the block diagram that was conceptualized for the Automatic Calibration System.

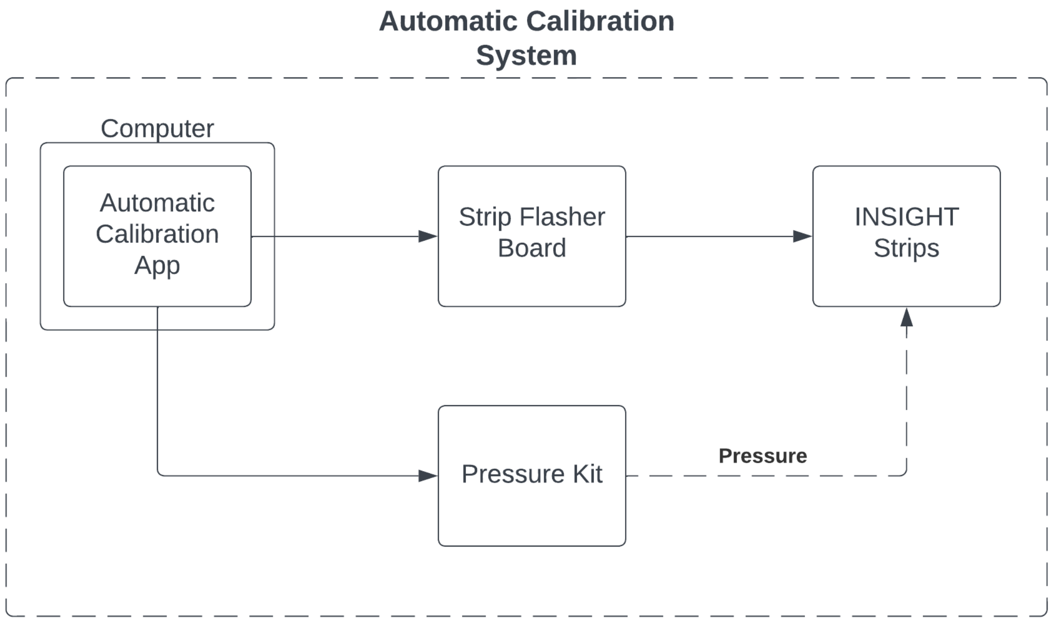

Figure 5.1: Automatic Calibration System Block Diagram

5.2 Initial System

During the initial stages of this project, a system was developed with a Command Line Interface (CLI). CLI is a text-based interface for interaction between the user and the system. This interface is renowned for its resource efficiency, lightweight nature and fast performance. However, the primary drawback of a Command Line Interface lies in its lack of user-friendliness.

The development of the initial system began with implementing the methods for controlling the Pressure Kit, starting with communication. Upon examining the manual system and consulting datasheets provided by manufacturers, it became evident that both the Pressure Regulator and pressure sensor relied on serial communication protocols utilizing COM ports. Serial communication is a protocol capable of transmitting data in a consecutive and sequential manner.

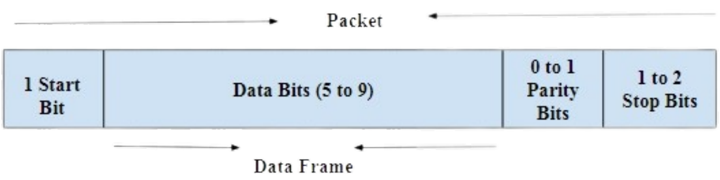

Figure 5.2: Standard bit structure for serial communication [22]

The standard bit structure for serial communication (Figure 5.2) consists of a start and stop character, from five to nine ASCII bits and the option of using a parity bit for error detection. Additionally, a Baud rate, which represents the number of pulses per second, needs to be specified.

For the Pressure Regulator, the maximum Baud rate supported is 9600 Baud. The datasheet also specifies the use of one stop bit, an eight-bit data frame, and no parity bit. To handle this communication, the Python module PySerial was implemented.

Regarding the pressure sensor communication, a Python module called pyLucidIO is provided by the manufacturer of the Analog-to-Digital Converter, Lucid Control. This module takes care of the communication and data acquisition.

To increase or decrease the pressure applied on the sensors, the system sends a target pressure to the regulator. Simultaneously, it monitors the change in pressure and waits until the pressure stabilizes within a specified tolerance range around the target pressure.

The following step is to acquire data from the INSIGHT™ sensors. The Strip Flasher Board also employs a serial communication protocol similar to the Pressure Regulator but with an increased Baud rate of 19200 Baud. Given that the Baud rate is the rate at which information is transferred in a communication channel it will reduce the time spent communicating with the Strip Flasher Board, in a factor of half compared to the Pressure Regulator, considering a message of the same size. Despite being advantageous for the automatic calibration system, the Pressure Regulator is not able of operating at faster Baud rates without loss of data.

After collecting the data at the relevant pressure steps, the system proceeds to determine the calibration parameters specific to each sensor using the methods described in Chapter 3.2.2.

To flash the microcontroller, an .hex file of containing the latest firmware is created. Additionally, for every strip, an .epp file is created containing all the data (ID, serial number, calibration parameters, etc.) that is to be saved in the EEPROM. One of the biggest challenges of this dissertation was in identifying which position of this .epp corresponded to which parameters as this was not documented. Furthermore, a memory error was occurring on the Wearable side of the system, causing positions of memory to be skipped on this .epp file. Investigating and correcting this issue required a significant amount of time, testing and team effort.

The flashing process involves the use of the AvrDude program, similar to the Strip Flasher App used in the manual calibration system (Section 4.2.2.1). However, in this case, the flashing process is integrated into the same application. This process simultaneously flashes the strips with the latest firmware and programs the *EEPROM* with the calibration parameters.

At this stage, the system was able to successfully calibrate and flash the strips, although it did not fully meet all the system requirements. It was tested on a Raspberry Pi to evaluate its compatibility and the conclusions drawn were that the system behaved identically on both platforms. Figure 5.3, shows the CLI interface running the Strip Calibration App.

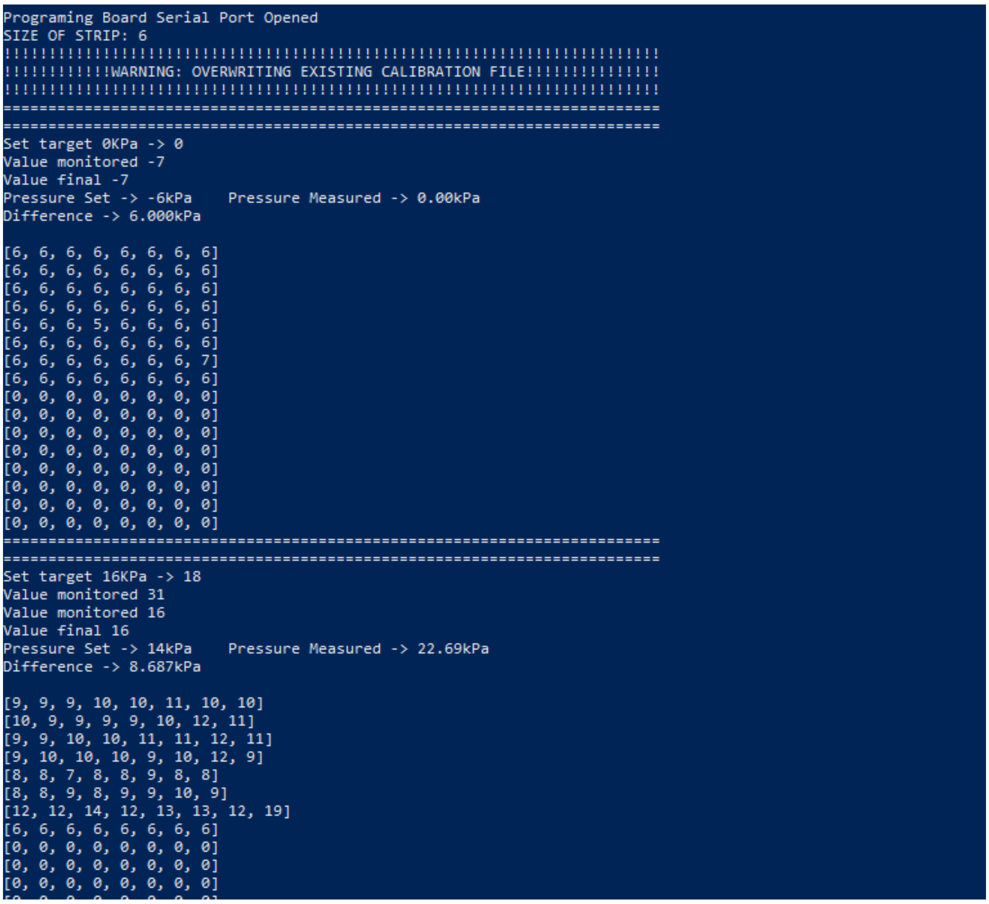

Figure 5.3: Command Line Interface of Initial System

Throughout the development of this initial version of the automatic calibration system, several challenges had to be overcomed. This challenges included technical issues with the firmware of the Strip Flasher Board and the INSIGHT™ Wearable. Investigating, identifying, and resolving these problems proved to be challenging and time-consuming. However, it provided a valuable opportunity to gain a better understanding of the INSIGHT™ system and other embedded systems.

As previously mentioned, not all the system requirements were fully met at this stage. An additional limitation of the initial system was the need to manually modify certain aspects of the code to adjust specific parameters. This practice, known as "hardcoding" in software development, was evident in various areas such as the COM ports used for serial communication with the Pressure Regulator, Sensor and Strip Flasher Board, as well as parameters associated with the pressure cycle. Most notably, this extended to the need of manually changing the parameters related to the flashing process of the strips, such as the number of sensors, strip ID, manufacturing date, and other relevant parameters.

Despite this, the initial system is capable of automatically performing the calibration and flashing the INSIGHT™ strips. The code structure is described in more detail in Section 5.4.

5.3 GUI System

To enhance user-friendliness, a Graphical User Interface (GUI) was developed using Python's *"Custom TKinter"* framework. GUI is a visual interface that uses graphical elements such as buttons, windows or menus allowing a more intuitive and user-friendly system. The downside of using a GUI is the use of more computer resources and increased complexity.

The main objective of the GUI's layout was to keep the process as simple as possible. With that in mind three windows were created.

The main window contains crucial information and allows the user to input parameters that change every time the calibration process is executed. As show in Figure 5.4, the user is able to input the Id of the first strip, the number of strips that are going to be calibrated (1-16) and the manufacturing date. Based on the Id of the first strip it deduces the number of sensors per strip (as explained before in Section 4.1.2) and displays that information for the user to verify. To obtain the Serial and Lot number and Firmware Version a .csv file containing information from all flashed strips is read. This .csv file works as a log that the system updates every time it executes. This is an extra feature that was added to keep a record of all the processed strips.

At this stage, the system executes a simple verification in order to not enable the user to surpass the IDs of said size strip, that is, if the ID of the first strip corresponds to a strip of size x the number of strips cannot be greater than the remaining IDs of size x. If this condition is not verified an error message is displayed and the number of strips is changed to the maximum allowed.

For the vast majority of times this is the only window the user will need to interact with. After pressing "Flash!" the calibration will start automatically. However some options might need to be changed.

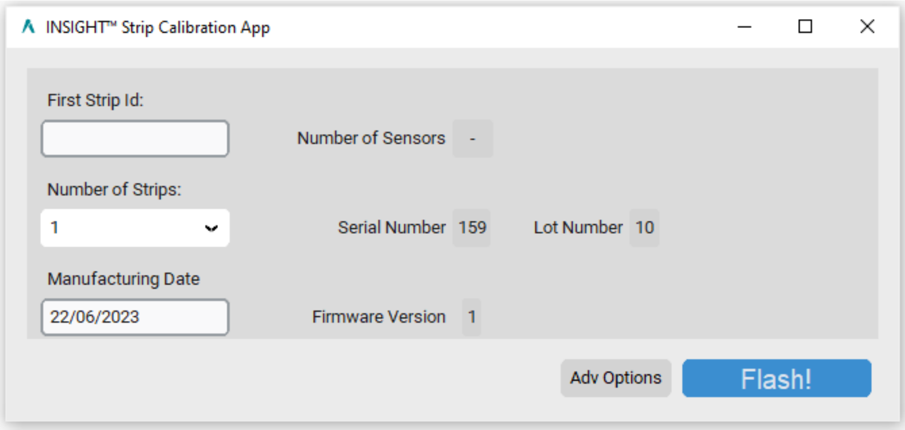

Figure 5.4: Main Window of GUI system

The Advanced Options Window , Figure 5.5a, allows to switch the pressure cycle from **Intake and Outtake**, **Intake** or **Outtake** and also the number of pressure cycles. For testing, research and development purposes the user may want the system to not use a valid serial number, to save .csv reports of ADC values at the pressure steps or to skip the calibration/flashing part of the process.

If hardware components change, so might the COM Ports, and for that the third and last window is used, Figure 5.5b. The window shows the default COM Ports for each component. These can be edited by clicking the drop down menu and selecting any of the available COM Ports. The user can then save the new COM Ports as default or simply exit only changing them for this calibration.

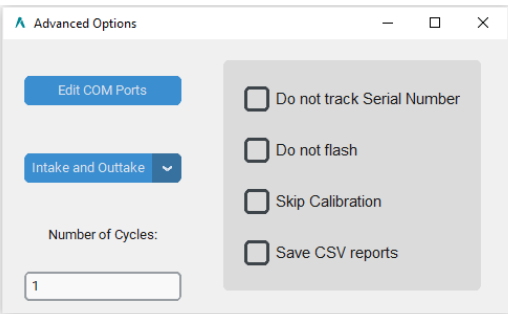

(a) Advanced Options window

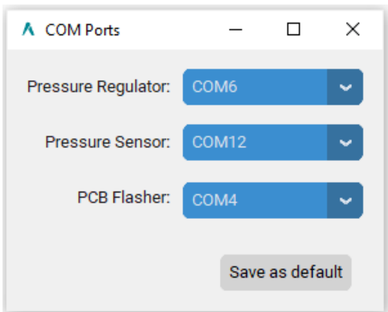

(b) COM port configuration window

Figure 5.5: Additional windows

At the end of the execution, the system reproduces a warning sound to alert the operator and a report is shown displaying either a success message if no error is encountered, Figure 5.6a, or an error message displaying the strips where errors where detected, Figure 5.6b.

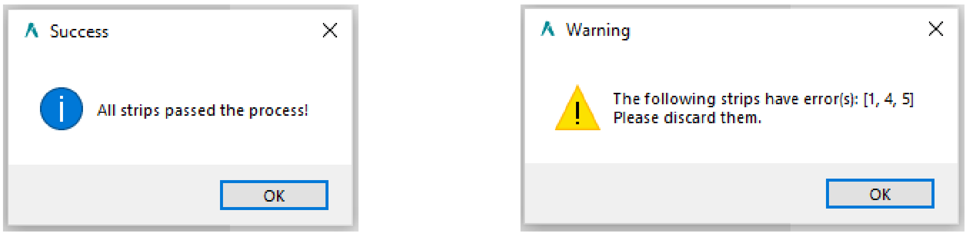

(a) Success Message (b) Error detecting message

Figure 5.6: Possible messages at the end of execution

5.4 Code Structure

For both cases, the code is structured similarly, only changing the user-system interface.

In Python, a module is a file that contains Python code, including variables, functions, and classes. This file may be imported and used by other Python applications, providing an approach to organize and reuse code, making it more straightforward to manage large projects and promote code reusability.

The Automatic Calibration System, developed in Python, is divided into seven modules, each serving a distinct segment of the code. Out of these seven modules, three are responsible for communication with the Pressure Regulator, Pressure Sensor and PCB. One for handling the flashing process, while three modules are dedicated to result processing, calculating the calibration parameters and handling the .csv files. The module breakdown is as follows:

- Communication modules:
  - Pressure Regulator Services
  - Pressure Sensor Services
  - Strip Flasher Board Services
- Flashing module:
  - Firmware Flasher
- Processing modules:
  - Results Processing Services
  - Calibration Services
  - CSV Services

This modular structure allows for a clear separation of responsibilities within the system. This simplifies code maintenance and updates as the code is more easily understood ultimately promoting code organization and reusability.

The flowchart of the Pressure Sensor Automatic Calibration System is represented in Figure 5.7

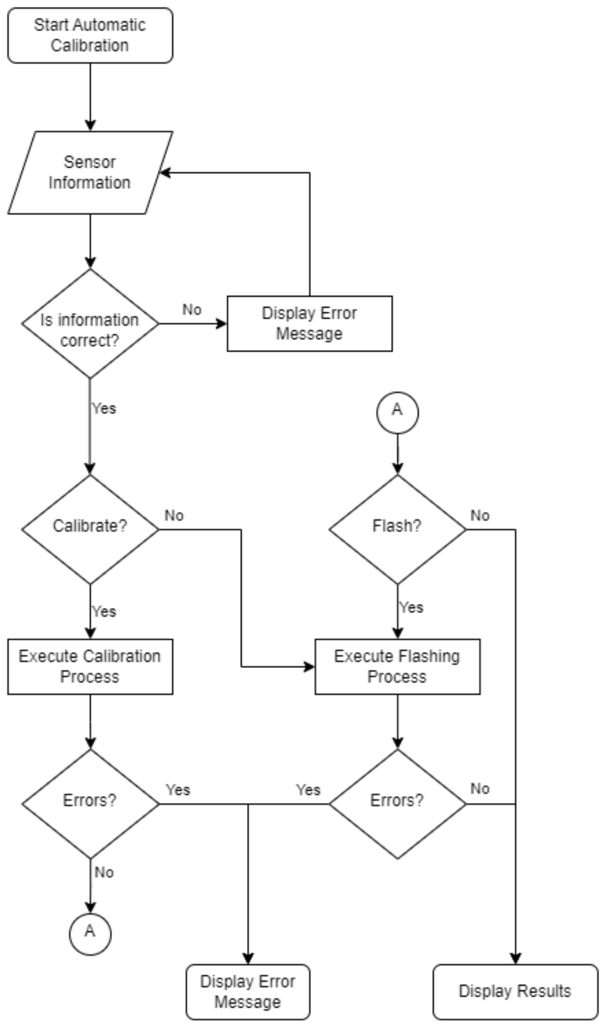

Figure 5.7: Flowchart of Automatic Calibration System

Throughout the execution of the system, multiple error verifications are performed at different stages. These tests are carried out to ensure a smooth operation and to detect and address any unexpected issues. These verifications aim to maintain the stability and reliability of the system. This is crucial given the fact that the system deals with high pressures and must release pressure if errors are detected to avoid unnecessary stress on components.

Initially, the information inputted by the user is checked and the flashing process only begins if everything is as expected. For instance, the operator is not allowed to input an invalid ID or chose to skip the calibration and flash in the same process as this means the system will not perform any task.

During the calibration process, the system automatically detects which strips were not connected, those that were disconnected midway or that where not connected from the beginning.

In addition, when processing the data collected, the response of each FSR sensor in each strip is evaluated against the requirements explained in Section 3.2.2.2.

Finally, during the flashing procedure, the occurrence of errors is also verified, primarily revolving around the flashing process itself, including potential issues regarding microcontroller responsiveness or communication errors.

All the errors previously described are not critical errors, but merely errors associated with a set of sensors or strips and, as such, the process continues to execute. However, the strips where errors were detected are ignored in the following stages. This implies that if a strip has a faulty sensor that is detected when calculating the calibration parameters the entire strip must be discarded. For this reason, that strip will not be flashed ensuring that serial number are not wasted.

There is, however, the possibility that the system encounters critical errors, specially associated with the serial communication between the computer and remaining components. Said critical errors result in the need to stop the code execution. For safety reasons, before stopping the code, the pressure is released from the pneumatic pressure and all communications closed.

Chapter 6

Complementary Work

The aim of this chapter is to shed light on complementary work performed alongside Adapttech®'s team, enabling the enrichment of this Master's dissertation and integration with the Embedded Systems team.

6.1 Study of the effect of the Air Vent on Force-Sensing Resistors accuracy

The development of a new system that enables continuous pressure distribution is currently being studied by Adapttech®. This could involve the development of a sensitized sock to be worn between the prosthetic liner and socket or the development of a smart liner with sensors incorporated. This would create the necessity of embedding sensors in fabric or silicone, greatly restricting the air vent. Even thought the function and importance of air vents on FSRs was introduced in the State-of-the-Art (Section 3.1.4), the actual impact resulting from their restriction or obstruction has not been adequately measured or evaluated. The correlation between restricted air vents and the resulting variations in measurement accuracy was determined through experimentation, data collection and analysis, providing a solid foundation for understanding the implications of sensor integration approaches and guide future design considerations.

Using calibrated sensors, a control test was performed on the pneumatic press without any restrictions on the air vent. A second set of tests was conducted, this time with the air vent restricted. The restriction of the airflow was attempted using three different methods:

- **Covering the air vent with silicone** — This first attempt failed for two reasons. Firstly, there was insufficient silicone on the air vent and the air pressure managed to penetrate through it. Secondly, using more silicone caused the layers of the FSR to separate, allowing the air to escape through several locations;
- **Coating the entire strip with silicone** — This approach was also unsuccessful. The layer of silicone covering the strip had to be very thin due to thickness of the pneumatic press

opening. Consequently, the silicone was not strong enough to withstand the force exerted by the air pressure;

- **Lining the strip with aluminium tape** — By covering the strip with robust aluminium tape, airtight conditions were successfully ensured to perform the tests (Figure 6.1);

The method using aluminium tape proves suitable for studying the effects of a restricted air vent. Further testing using thicker layer of silicon can be relevant, but in that case, a new pressure testing device would need to be constructed to accommodate thicker strips. As a proof of concept, a manual device was conceptualized using old parts and a load cell to create a clamp capable of providing pressure readings. The construction of this device was completed by Adapttech®'s mechanical team, however, it was not possible to validate it in time to conduct the desired tests.

The first two attempts, despite having failed, enabled some conclusions to be drawn, the main being that the current sensors could not withstand high pressures with the air vent covered. This phenomenon occurs due to the high pressure exerted by the pneumatic press on the strip, which results in the transmission of that pressure to the layers of the sensor. The restricted airflow prevents the air from escaping, causing the pressure to be applied on the layers of the sensors leading to layer separation.

Figure 6.1: INSIGHT™ Sensor covered with aluminium tape

6.1.1 Results

When airtight conditions are ensured, it is expected that the output of the FSR undergoes significant attenuation. As the pressure exerted on the strip by the pneumatic press increases, the trapped air is not able to escape and begins to compress, resulting in resistance against the press. This compression and resistance cause substantial attenuation of the FSR output.

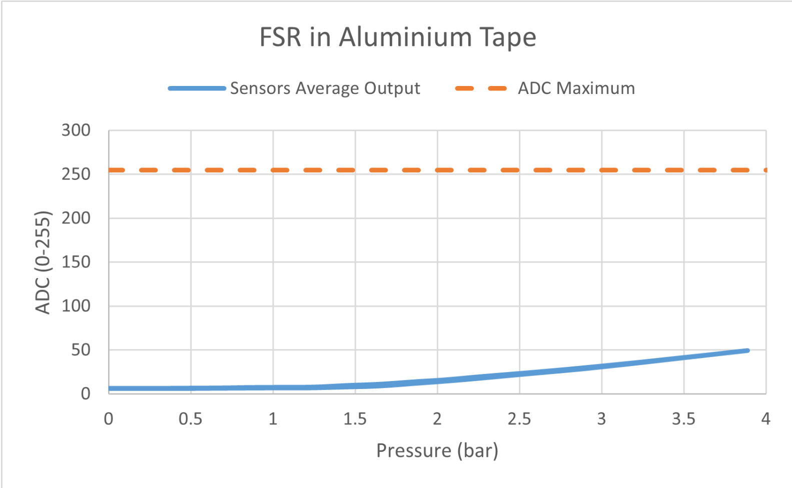

(a)

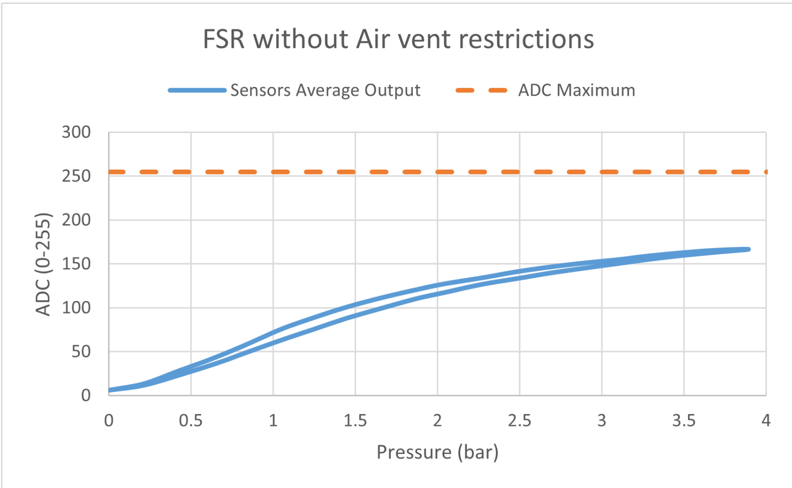

(b)

Figure 6.2: (**a**) Response of restricted FSR, (**b**) Response of unrestricted FSR

Figure 6.2 clearly illustrates the effect of a restricted air vent. A FSR operating under airtight conditions, has an ADC reading approximately ranging from 0 to 50 as the pressure varies from 0 to 3.8 bar. In comparison, when the air vent is unrestricted, the ADC range approximately spans from 0 to 165, this represents a 70% decrease. With such a limited range, precision is compromised. Based on this findings, it can be concluded that the sensors currently being used are not suited for embedding in fabric, silicone or use in other airtight applications.

6.1.2 Testing Different Sensors

There are, however, alternative sensors that do not require an air vent. Several relevant sensors were tested, although specific details regarding certain sensors, tests, and results must remain confidential.

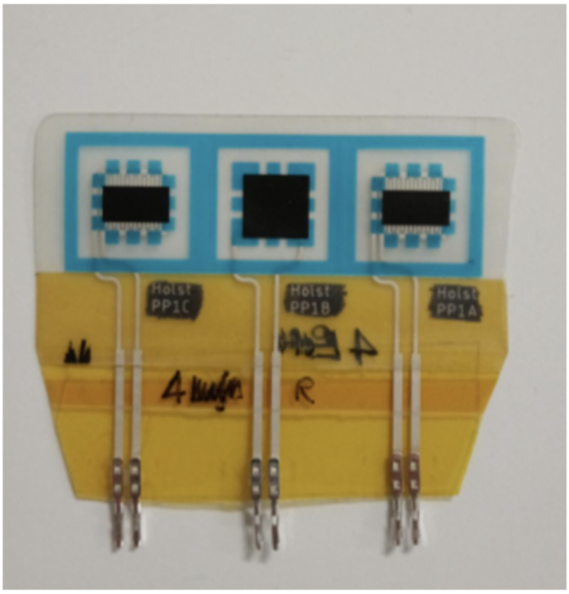

Figure 6.3: Three different Force-Sensing Resistors configurations with air pocket

One alternative that was tested is a FSR sensor by TNO. In contrast to traditional FSRs that rely on an air vent, this particular sensor design incorporates pockets or cavities that allow air to escape and expand within them (Figure 6.3). Three different sensors with three different configurations and resistance values were tested. While this approach is interesting, it presents two major drawbacks in Adapttech®'s case. Firstly the air pocket is effective only if it is not under pressure, which means that the pocket of air needs to be outside the contact zone between the limb and the socket. Secondly, this approach is significantly impacted by hysteresis due to the dependence of air pocket elasticity on the separation of FSR layers.

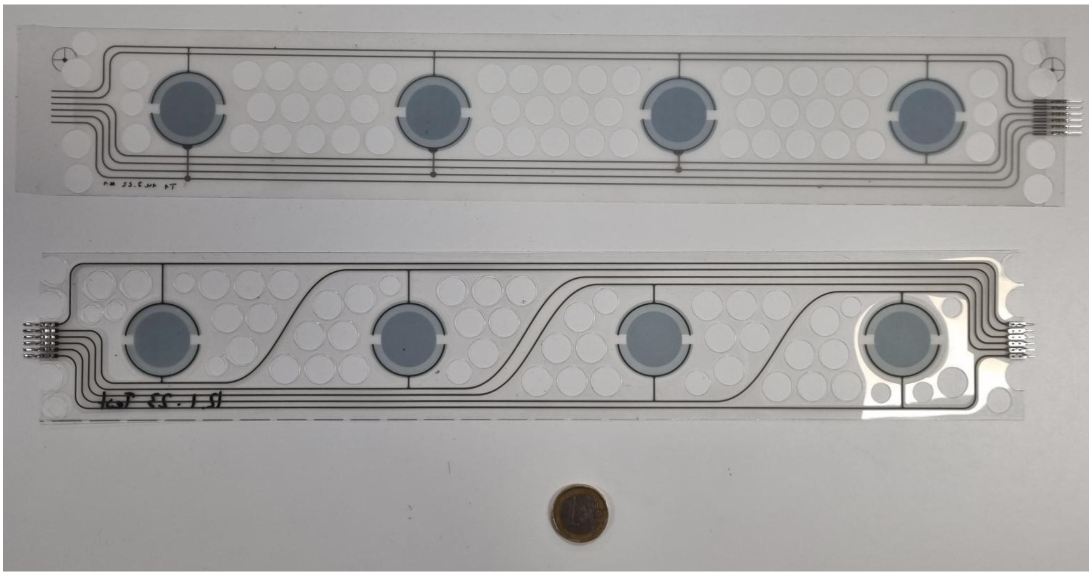

Figure 6.4: Two samples of Piezoelectric pressure sensors

Another sensor that was tested was a piezoelectric sensor (Figure 6.4), whose working principle is further elaborated in 3.1.5. Piezoelectric sensors are sensors that convert pressure changes into voltage through the piezoelectric effect. These sensors offer various advantages for this type of application, such as absence of moving parts, thin and flexible form factors and no requirement for an air vent. However, their primary drawback is the fact that they have a dynamic nature, this means that they only respond to changes of force. Consider a scenario where a 10Kg weight is placed on top of the sensor. Upon dropping the weight onto the sensor, a voltage spike is generated, which subsequently returns to zero volts. In our case, the goals is to measure both dynamic and static pressure situations while consistently capturing the total pressure, rather than changes in pressure alone. While it is possible to calculate the total pressure using well-designed circuits or post-processing techniques, this approach is resource-intensive and does not yield the most reliable results. Additionally, even for testing purposes more complex circuits are needed for using this sensors, namely acquisition circuits with high input impedance.

Various technologies were tested, but specific details regarding these technologies cannot be disclosed at this time.

6.2 INSIGHT™ Sensors Improvements

Despite offering innovative features and significantly improving the quality of life for lower limb prosthesis users, the INSIGHT™ Sensors have a notable drawback: its usage times is inherently limited, with the recommended number of uses being limited to eight times.

Under the current circumstances, after the recommended number of uses, the strips are discarded resulting in a significant amount of electronic waste. Reducing this e-waste has become a priority for Adapttech®, and the idea of reusing the PCB present on the strips while replacing the remaining components has been considered. However, achieving this goal is a complex task.

The circuitry present in the PCB, as discussed in Section 4.1.1, was initially developed with different sensors in mind, involving a large number of components. Furthermore, difficulties related to poor connection between the strips and the PCB have frequently been encountered. Since the connection between PCB and Strip is made through very thin pads, misalignment and inadequate adhesion can lead to the failure of certain sensors or even the entire strip. In both cases, the strips have to be disposed of.

Considering the aforementioned reasons, it has become necessary to design and study a new PCB that addresses these challenges.

6.2.1 INSIGHT™ Sensors- Second Generation

The first generation of INSIGHT™ Sensors use an 8-bit, 8-channel Analog-to-Digital Converter along with a separate microcontroller (Section 4.1.1). It is important to note that this microcontroller does not perform any processing task, its sole responsibility being to store unique information and the calibration parameters of the sensors. The ADC and microcontroller are independent entities and cannot communicate with one another, as they are only connected to the USB-C interface. The only upside to this approach is that the ADC can function regardless of the microcontroller's state.

However, this configuration represents an inefficient use of processing power and incurs unnecessary expenses, considering that the microcontroller purely has the function of an EEPROM memory.

Furthermore, the signal Processing Circuit employs eight op-amps in Integrated Circuits (IC) of two op-amps and several passive components such as resistors and capacitors. Altogether, including the AVR microcontroller, Analog-to-Digital Converter, signal Processing Circuits and the remainder of the components, this iteration integrates six active components and twenty-nine passive components.

A more appropriate approach would involve using a microcontroller equipped with an internal ADC that complies with the system requirements. The primary requirement is a minimum time between samples of 20 milliseconds, ensuring that the prosthetist has access to relevant data at any given moment. Several alternatives were evaluated, ultimately leading to the selection of the ATtiny-1626 microcontroller, by Microchip. This relatively inexpensive microcontroller belongs to the tinyAVR family, offering adequate processing power and featuring a 12-bit, 15-channel Analog-to-Digital Converter.

With the implementation of the ATtiny-1626, the second generation significantly improves compared to the first generation. Notably, the Analog-to-Digital Converter exhibits enhanced capabilities, with the resolution increased from 8-bit to 12-bit. The number of channels has also been expanded from 8 to 15. Even though currently only eight channels are necessary, this design allows for seamless integration of additional sensors in the future, if the need arises. Relative to the speed the new ADC has a rated conversion rate of 375 ksps (kilosamples per second) versus a conversion rate that could range from 200 ksps to 500 ksps of the previous converter.

The signal Processing Circuit also underwent revisions in order to improve the output and reduce the number of components. As previously mentioned, the first generation INSIGHT™ Sensors were designed for a different sensor type than that of the ones currently being used. For the FSRs implemented at the moment, the circuit with the op-amp becomes unnecessary. Non-inverting amplifiers are typically employed in applications that require high input impedance, which is not the case for FSR sensors. Additionally, signal amplification is also not required for these sensors. An alternative approach is to implement a resistive voltage divider, which confers simplicity and resource efficiency.

A resistive voltage divider is the most common type of voltage dividers, a type of electronic circuit used to obtain a voltage that is a fraction of the input voltage (Figure 6.5). This circuit consisting of two resistors in series, and can be used to determine the pressure on the FSR. The output voltage can be calculated using equation 6.1.

$$V_{out} = V_{in} \times \frac{R_2}{R_{FSR} + R_2} \tag{6.1}$$

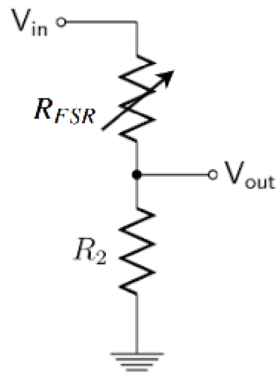

Figure 6.5: Voltage divider circuit

In order to study the accuracy and conduct multiple tests, a test circuit (Figure 6.6) was assembled using a ATtiny-1626 development board, enabling comprehensive analysis and comparison with the existing method. In this application, each individual FSR is represented by R_{FSR} and is in series with another resistor. The goal of this test is to evaluate the best value for R_2 resistor and also reference voltage. The ADC converts the voltage into a value from 0 to 4095 since it has a resolution of 12-bit. The ATtiny then performs a downsampling to a scale from 0 to 255 in order to use a single byte in the communication. This aspect is something that would be changed if this systems is to be implemented, to increase precision. However this would involve some changes in software, so for testing purposes the signal was downsampled. The ATtiny is connected to a Arduino using SPI communication protocol. The objective is to use as much as the range of the ADC in the test pressure range (from 0 to 3.8 bar) without saturating the sensors, ensuring good resolution and precision.

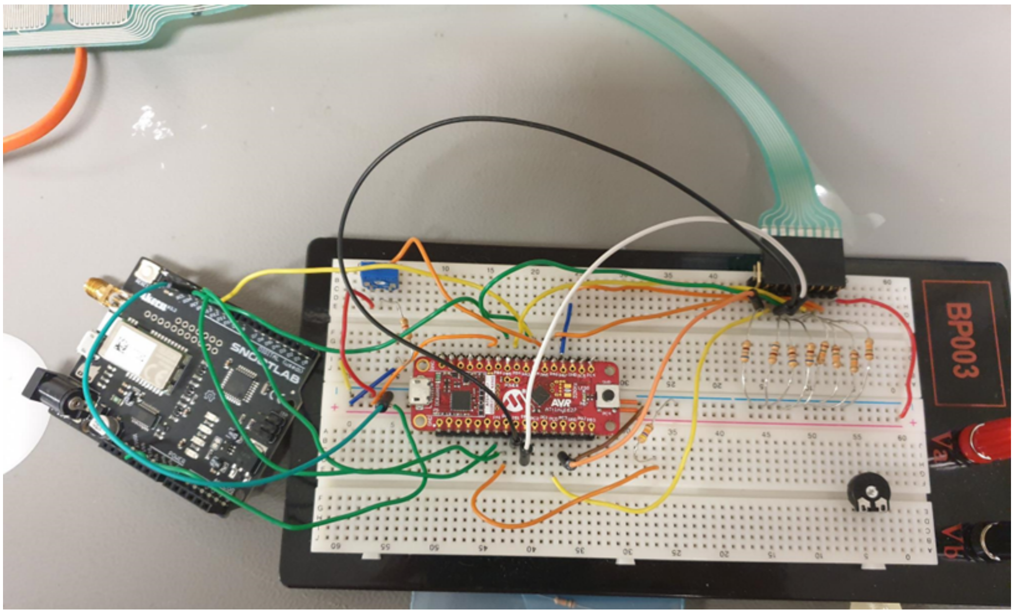

Figure 6.6: Test circuit for comparing different FSRs with voltage divider

In the experimentation phase, several samples of Force-Sensing Resistorss with different characteristics and resistance were tested. This tests involved using different resistors in series with the sensor and also distinct reference voltages. While some specific details of these tests are confidential, focusing on two samples: sample *B* and sample *C* with with different intrinsic resistance magnitudes.

Denoting $R_{intrinsicB} \ll R_{intrinsicC}$ as the intrinsic resistance of sample B and C respectively, $Vb_{ref1} < Vb_{ref2}$ as two reference voltages of the ADC for sample B with orders of magnitude of 0 (V), R_b a series resistor for sample B with order of magnitude of 3 (Ω), Vc_{ref} the reference voltage for sample B with order of magnitude of 0 (V), $R_{c1} < R_{c2}$ two series resistors for sample C with orders of magnitude of 4 (Ω).

The combination of these parameters affects the response of the ADC. Both samples were tested with the previous calibration system in similar conditions, yielding the following results.

Sample B (Figure 6.7) exhibits a logarithmic response with the influence of the reference voltage being evident. Increasing the reference voltage raises the maximum voltage the Analog-to-Digital Converter input can withstand before saturation. Therefore, the combination of sample B, R_b with the Vb_{ref2} saturates at higher pressure values, around 3.4 bar, compared to the combination with the lower reference voltage Vb_{ref1}, which saturates at a significantly lower pressure of 3 bar.

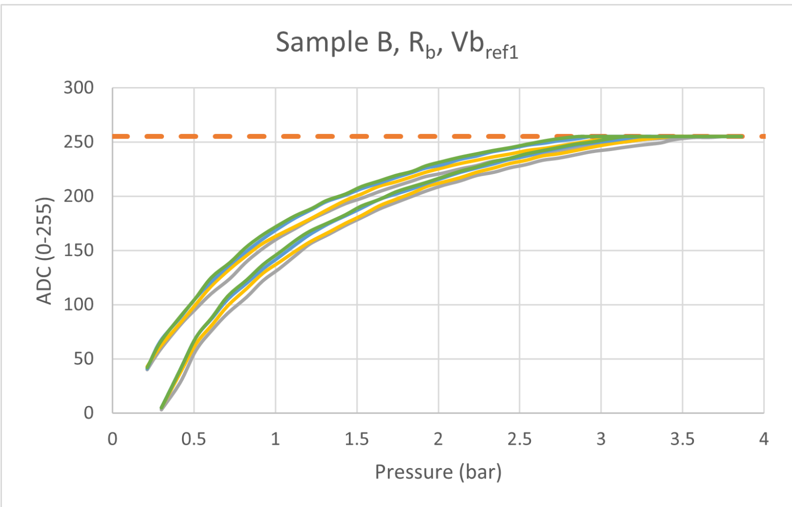

(a)

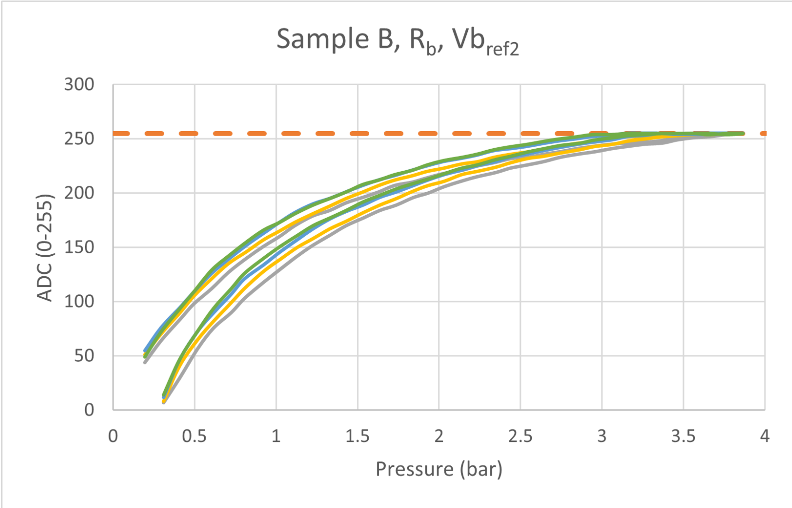

(b)

Figure 6.7: Sample B tests with R_b, (**a**):Vb_{ref1} or (**b**):Vb_{ref2}

Sample C (Figure 6.8) demonstrates a more linear response. In this case, the effect of changing the resistor in series with the FSR is studied. The voltage on the input of the ADC is given by equation 6.1. Increasing R_2 leads to an increase in V_{out}. Consequently, the combination of sample C, R_{c2} and Vc_{ref} produces a higher output that saturates at around the highest pressure values compared to the combination with the lower series resistor R_{c1}, which does not reach saturation within the tested pressure range. In comparison with the first generation, this combination of FSR, resistor and reference voltage enables the use of the full range of the ADC, increasing precision of the entire system.

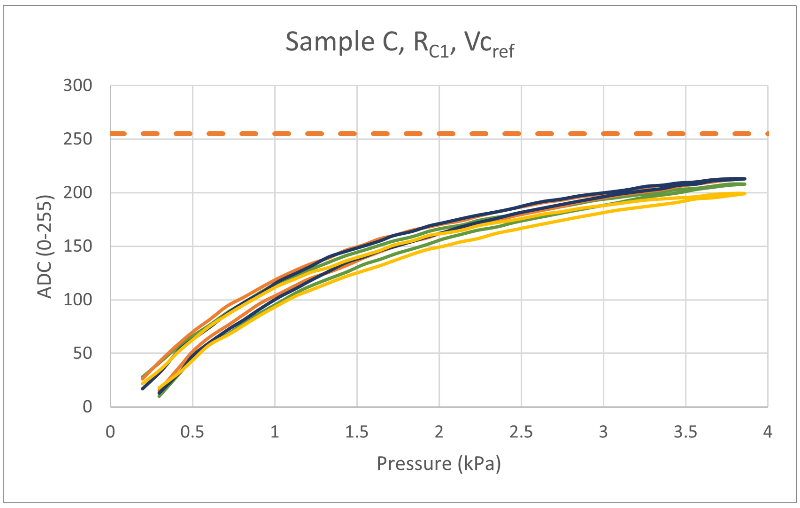

(a)

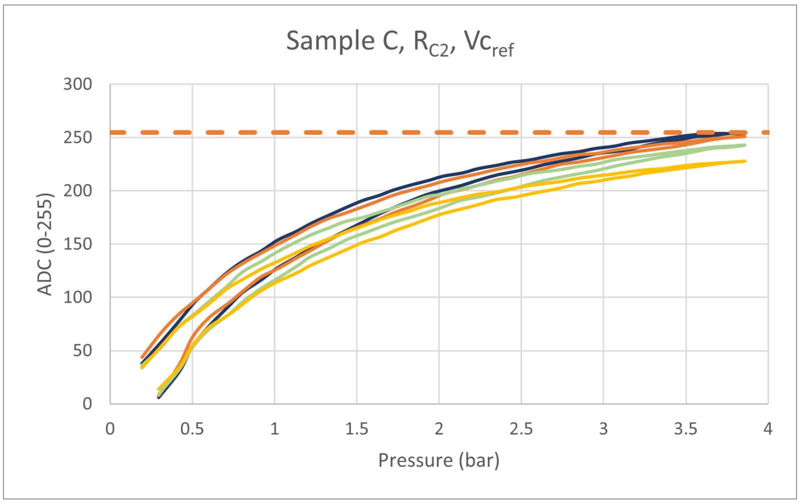

(b)

Figure 6.8: Sample C tests with Vc_{ref}, (**a**):R_{c1} or (**b**):R_{c2} and

The more linear response of sample C is a significant advantage. However, this sample of sensors presents one major drawback. Due to the significantly higher intrinsic resistance of sample C compared to sample B, an inter-sensor variation similar in percentage has a greater impact on the sample with higher resistance. Achieving the ability of using the same calibration for every sensor is an intriguing possibility for the future of Adapttech®. Therefore, the chosen combination is sample B with a reference voltage (V_{ref}) close to Vb_{ref2}. To further converge the response of the sample B sensors, low tolerance resistors were implemented.

The ADC of the microcontrollers offers five internal reference voltages (supply voltage plus four additional preset voltages) or the resource to use an external reference. While using internal voltages would be advantageous in terms of reducing electronic waste, tests concluded that an external reference voltage would enhance precision. This external voltage reference is obtained utilizing a voltage divider.

The PCB for the second generation INSIGHT™ Sensors was design using Altium Designer, by Adapttech®'s embedded systems team, with a simpler and improved layout. The first test version uses wider copper pads for connecting with the sensors to improve the quality of the connection. Further on, the use of connectors like Flexible Printed Circuit (FPC) connectors will be studied and if proven feasible implemented. This type of connectors greatly improve the recycling process, however they must be capable of withstanding the tension caused by regular use.

Comparing with the first generation, the second generation PCB (Figure 6.9) is more organized, uses less components and less expensive to manufacture. With a decrease in the number of components it became possible to fit all the components on the upper layer, this further lowers the costs, around 50%, and makes the PCB assembly thinner. Additionally since this second generation has refurbish in mind, the new plastic cover uses screws instead of glue to ensure they can be used multiple times. Unfortunately the new PCB did not arrive in the given time frame so it was not possible to study and evaluate it's performance.

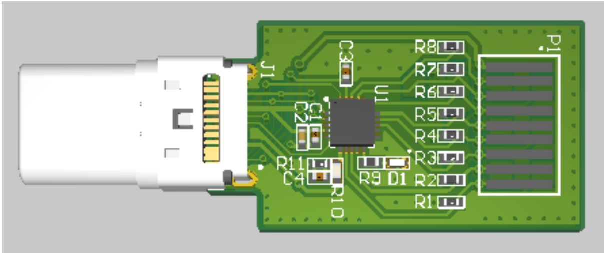

Figure 6.9: 2^{nd} Generation INSIGHT™ Sensors PCB

Table 6.1 displays the most important changes between first and second generation INSIGHT™ Sensors.

Table 6.1: Comparison table between generations

	First Generation	Second Generation
Active Components	6	1
Passive Components	29	16
ADC Resolution	8-bit	12-bit

Chapter 7

Results

In this chapter, the Pressure Sensor Automatic Calibration System is tested an analyzed. It begins with an overview of the system, followed by a discussion of the calibration results. Finally, a comparison is made between the new automatic system and the previous manual system, both in terms of time performance and of usability.

7.1 Overview

The Pressure Sensor Automatic Calibration System was able to fully meet both functional and non-functional system requirements outlined in Section 5.1. The system is capable of accurately flashing and calibrating the strips, detecting errors, and evaluating calibration parameters. Several features were incorporated to allow important tests for sensor evaluation. The Graphic User Interface was developed with user friendliness in mind.

Furthermore, additional functionalities have been implemented, such as automatic logging of serial and Lot numbers, eliminating the need for manual entry by the user.

7.2 Calibration Results

As previously explained in Chapter 3.2.2, the primary objective of the calibration is to linearize the output of the sensors and extend it to the full scale of the Analog-to-Digital Converter.

The system autonomously performed the calibration of eight large strips, each containing eight sensors. Out of the total sixty-four sensors subjected to calibration, three failed the calibration, while the remaining passed the calibration successfully. For evaluation purposes, three randomly selected sensors from the successfully calibrated group and the three sensors whose calibration failed were chosen. The calibration results of these six sensors are presented below.

Figures 7.1a, 7.1b and 7.1c depict the accepted calibrations. The blue dots represent the response prior to the calibration, while the orange dots represent the response after the calibration. The black line represents the ideal response, while the two dotted orange lines indicate the upper and lower ADC thresholds. The maximum value of the ADC is 255 and 6 is the lowest value the ADC reports if connected to the Force-Sensing Resistors.

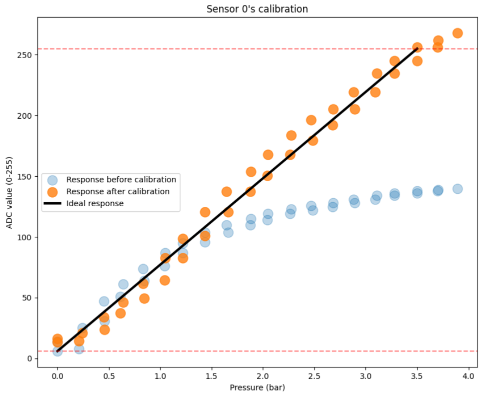

(a) Calibration of Sensor 0

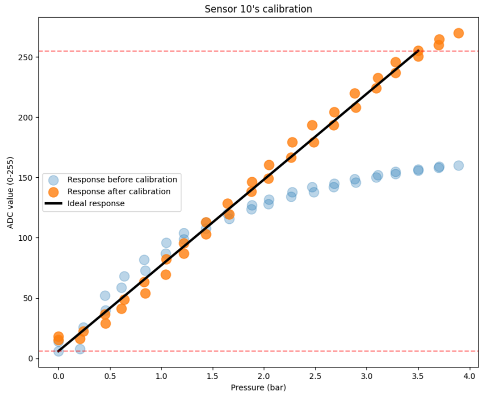

(b) Calibration of Sensor 10

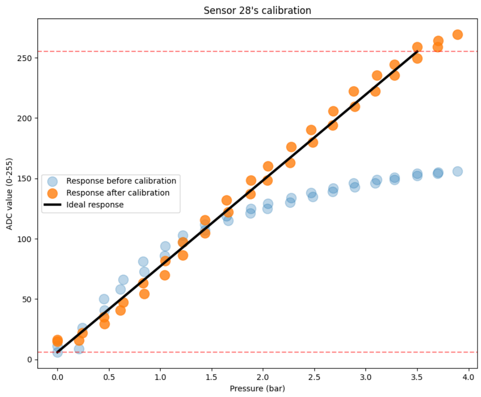

(c) Calibration of Sensor 28

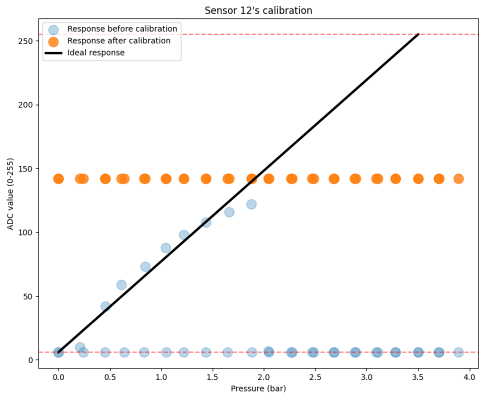

(d) Calibration of Sensor 12

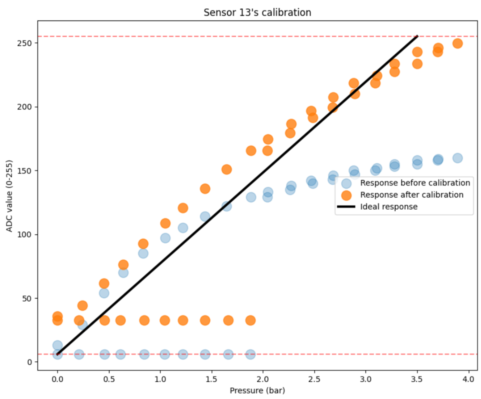

(e) Calibration of Sensor 13

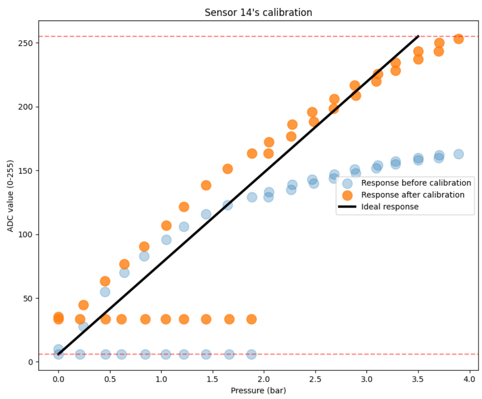

(f) Calibration of Sensor 14

Figure 7.1: Accepted calibrations **(a) (b) (c)**, and failed calibrations **(d) (e) (f)**

The response without calibration exhibits a logarithmic form and a value at the ADC of approximately 150 at 3.5 bar. After the calibration is applied, the response is nearly linear, with minimal hysteresis. The maximum of the ADC is achieved at 3.5 bar, which corresponds to the maximum expected pressure inside the socket, as discussed in Section 3.2.2.

On the other hand, figures 7.1d, 7.1e and 7.1f represent rejected calibrations. Upon analyzing these plots, it can be concluded that all three sensors exhibited poor connection with the sensor PCB. In the cases of sensor 13 and 14, the connection improved during the intake phase as the process reached 2 bar. For sensor 12, the improvement occurred significantly later during the outtake phase of the pressure cycle. In both cases, the three sensors failed the calibration process. Specifically, sensor 12, 13, and 14 were all part of the strip with ID 2, which had to be discarded accordingly.

7.3 Time comparison between Automatic Calibration System and Manual Calibration System

When comparing the new Automatic Calibration System with the Manual Calibration System, two important time metrics are considered: the total time taken by the system to complete the process and the time the operator needs to be present for the system to function.

To assess the time difference, a member of the Biomedical team from Adapttech®, referred to as Subject A, was selected to perform the flashing and calibration process using both the new and old systems. This choice is justified given the fact that subject A is familiarized with the old calibration system and is regularly involved in the flashing and calibrating tasks. Subject A was timed performing the flashing and calibration process of eight large INSIGHT™ sensors.

Table 7.1: Comparison of times with experience user

	Time user is required	Total time
Manual Calibration System	15:01 minutes	16:10 minutes
Automatic Calibration System	02:35 minutes	12:06 minutes

Table 7.1 presents a comparison between the automatic and manual calibration systems. The one minute and nine seconds difference between the total time and user time in the manual system represents the time taken for flashing the microcontrollers, during which the user is not actively engaged. Typically, this time is utilized for preparing for the subsequent steps of the process.

The new system outperformed the manual system in both categories, total time and user time. It was four minutes and four seconds faster in total time. More significantly, it reduced the time required for the operator to be present and attentive by twelve minutes and twenty-six seconds. This translates to an 83% reduction in user time and a 25% decrease in total time. The system successfully flashed and calibrated seven strips, with one strip discarded due to unresponsive sensors.

7.4 Usability of the Automatic Calibration System

As discussed in Section 5.3 the Graphic User Interface was designed to prioritize simplicity and user-friendliness.. To evaluate the usability of the system, two members of Adapttech® who were not regularly involved in the calibration process and had no prior exposure to the new system were given instructions and timed to assess their understanding and interaction with the interface. The test conditions were similar to those in the previous evaluation. The instructions given to the subjects were as follows:

1. Insert 8 large strips on the press and connect them to the Strip Flasher Board;
2. Launch the Automatic Calibration System application
3. Flash the strips with the following parameters:
    - First Strip Id: 1
    - Number of strips: 8
    - Manufacturing date: 21/06/2023

The test results, Table 7.2, yielded interesting observations. Both test subjects performed faster than the test subject from Section 7.3. It is important to note that Subject B did not execute a successful calibration and flashing process. Subject B was unaware that the strips, lacking a plastic casing, cannot be twisted to ensure proper connection. Consequently, all eight strips failed the calibration. Since the calibration failed in all strips, the flashing process was not performed. This is a feature that is implemented to ensure that serial number are not used in faulty sensors. This resulted in a quicker completion of the overall process, but can't be compared to the total time of the other subjects.

Table 7.2: Comparison of times with experience user

	Time user is required	Total time
Subject B	01:56 minutes	10:35 minutes
Subject C	02:06 minutes	11:46 minutes

Subject C, being instructed to pay more attention to the positioning of the strips to avoid repeating the mistakes of Subject B, achieved the same results as Subject A, with seven successful calibrations and one strip encountering the same error as encountered in Section 7.3. Subject C performed approximately twenty to thirty seconds faster than the experienced subject in both metrics.

These results emphasize the significance of handling and positioning the strips correctly during calibration.

7.5 Conclusions

The results obtained from testing the Automatic Calibration System demonstrated significant improvements in the flashing and calibration process. The time spent by an operator performing these tasks was greatly reduced.

Having observed subject A, B, and C, it is possible to conclude that the extra time that subject A required to execute the task was attributed to a meticulous attention to detail, ensuring the generation of accurate and precise results. This extra time was not due to an adaptation period, as the application had previously been introduced to the subject.

For this reason and based on feedback from the users, it can be concluded that the new system does not require a substantial familiarization period and all subject were able to quickly and correctly configure the application to perform the specified tasks. It is important to note that for more complex tasks, such as sensor characterization, the same principles apply, however this task requires a subject that is familiar with the system.

The system has proven its capability in ensuring that the time of operators can be employed in more useful ways. The positive outcomes obtained from the testing phase support the conclusion that the Pressure Sensor Automatic Calibration System is a reliable and valuable asset in the company for which it was developed.

Chapter 8

Conclusion and Future Work

The present Master's Dissertation aimed to develop a new and automatic system capable of calibrating Force-Sensing Resistors and flashing a microcontroller used as an interface between the system and the sensors. This chapter provides an overview of the developed system, the obtained results, and a comparison between the system requirements and the final outcome. Additionally, the chapter covers complementary work conducted and suggestions for further enhancing the system.

8.1 Conclusion

Numerous types of pressure sensors where studied and even tested, with distinctive characteristics and applications. Despite the drawbacks mentioned and evaluated, as of this moment, Force-Sensing Resistors are still the best option to incorporate in Adapttech® INSIGHT™ system, due to their availability, competitive price and flexibility. Additionally, the fact that they do not require a complex Processing Circuit and that when accurately calibrated produce reliable results is an important advantage for this system. Nevertheless, technological advancements and Adapttech®'s continuous pursuit for improvement, might motivate a change in the type of sensors used in this application or the development of a completely new product. The pursuit of excellence and innovation has positioned Adapttech® as a prominent player within the industry.

Gaining familiarity with the INSIGHT™ system and the manual calibration process was within the scope of the project, which enabled the development of the Automatic Calibration System to meet the needs of both the system and the operator. The developed system successfully fulfills all the system requirements. The system operates as efficiently and as autonomously as currently possible, only requiring the operator to do initial configurations. As a consequence of extensive testing, the system is capable of detecting and dealing with countless errors, and most importantly it produces accurate and reliable calibrations.

Considering the collected data described in Chapter 7, it is evident that the system drastically reduced the duration of operator involvement. It is also clear that an inexperienced operator can obtain satisfactory results if given the correct instructions. Thereby concluding that the Pressure

Sensor Automatic Calibration System has successfully accomplish its main goal of improving the efficiency of operator time while maintaining a simple yet comprehensive interface. Reducing the human intervention also lowers the probability of errors occurring which was significant in the manual system.

This past months working in conjunction with Adapttech® have created numerous learning opportunities not only in areas related to this dissertations but in different fields. The complementary work described in Chapter 6 allowed the enrichment of knowledge in the field of electronics and embedded system but also problem solving and prototyping skills. Most importantly, the collaborative teamwork environment enabled a better understanding of effective collaboration and communication, of how every moving part contributes to the bigger picture, and also familiarization with Scrum methodologies.

8.2 Future Work

During the development and testing phases of the system, extensive discussions were held regarding additional features and improvements. As a result, certain features were successfully incorporated and others have been identified for potential future implementation, based on their relevance and significance.

When a sensor is discarded during any stage of the process, it is set aside to later be evaluated, when a significant number of discarded sensors has been gathered. There are two possible outcomes for a sensor depending on the factor that caused their rejection. If a sensor presents a major fault, it is considered as electronic waste. However, it is possible that the fault is fixable and that, after rework, the sensor is no longer defective. As a result of sensor discarding, per calibration batch, a random assortment of sensors is generated with varying sizes and nonconsecutive IDs. To help with processing this assortment of sensors, a feature could be added to allow the system to process strips of various size and nonconsecutive Ids.

For quality assurance purposes, an additional feature could be implemented. This feature would generate or update reports each time the system encountered a defective sensor. These reports would contain information regarding common causes of failure and the frequency of their occurrence. This would enable quality assurance technicians to detected any change of trend and evaluate it. For example, it would be possible to identify an increased number of sensors with defects, indicating a potential manufacturing problem. Another valuable parameter that could be added to the Automatic Calibration System is the ability to identify the operator who performed the calibration process. This information could be added to the existing system log, providing insights into quality control, performance, and training needs.

In some cases it may be desirable not to flash the strips with the latest firmware but instead use a test or showcase firmware version, with features adapted to its use case. In the future, the system could offer the option to select from multiple available firmware versions.

The Automatic Calibration system could be integrated with a Network-Attached Storage (NAS) system, enabling a copy of the logs and firmware to be available to the entire network rather than just locally.

One aspect that was not thoroughly tested was the performance of the system when implemented on a network-enabled single board embedded computer with an attached touchscreen, such as a Raspberry Pi. Overall, the system does not require a lot of processing power with the exception of the calculations for obtaining m and b. Also the communications seemed to take longer when the Initial System was tested on the Raspberry Pi. This might slow the performance of the system. Although the system is compatible with this family of single-board computer, some minor changes might be necessary to ensure a efficient and reliable performance. Due to technical difficulties and time constraints, this aspect could not be concluded in the scope of this dissertation.

Regarding future applications, this system could be used with minimal modifications for different sensors with similar working principles. The system can also accommodate for changes in sensors that require different processing circuits, such as piezoelectric sensors. With significant changes, the system could potentially be adapted for a different product, such as a smart liner, for example.

References

[1] Kathryn Ziegler-Graham, Ellen J MacKenzie, Patti L Ephraim, Thomas G Travison, and Ron Brookmeyer. Estimating the prevalence of limb loss in the united states: 2005 to 2050. *Archives of physical medicine and rehabilitation*, 89(3):422–429, 2008.

[2] Samreen Hussain, Sarmad Shams, and Saad Khan. *Impact of Medical Advancement: Prostheses*. 11 2019. doi:10.5772/intechopen.86602.

[3] Moss Rehab. Lower extremity amputation types & levels, 2023. Accessed on January 03, 2023. URL: https://www.mossrehab.com/amputation-and-prosthetics/lower-extremity-amputation.

[4] Infinite Technologies. Above knee leg prosthetics, 2017. Accessed on January 03, 2023. URL: https://www.infinitetech.org/above-knee-leg-prosthetics/.

[5] Ebrahim A Al-Fakih, Noor Azuan Abu Osman, and Faisal Rafiq Mahmad Adikan. Techniques for interface stress measurements within prosthetic sockets of transtibial amputees: A review of the past 50 years of research. *Sensors*, 16(7):1119, 2016.

[6] Adapttech Ltd., 2023. Accessed on January 04, 2023. URL: https://www.adapttech.eu/.

[7] MAAS Collection, 2014. Accessed on June 29, 2023. URL: https://ma.as/525134.

[8] Ottobock. How liners work, 2023. Accessed on January 07, 2023. URL: https://www.ottobock.com/en-gb/how-liners-work.

[9] Tekscan. F-scan system. Accessed on January 08, 2023. URL: https://www.tekscan.com/products-solutions/systems/f-scan-system.

[10] Tekscan. F-socket system, n.d. Accessed on January 08, 2023. URL: https://www.tekscan.com/products-solutions/systems/f-socket-system.

[11] Ted Nachazel. What is a strain gauge and how does it work?, 2020. Accessed on January 08, 2023. URL: https://www.michsci.com/what-is-a-strain-gauge/.

[12] Ebrahim Al-Fakih, Noor Abu Osman, and Faisal Mahmad Adikan. Techniques for interface stress measurements within prosthetic sockets of transtibial amputees: A review of the past 50 years of research. *Sensors*, 16(7):1119, Jul 2016. URL: http://dx.doi.org/10.3390/s16071119, doi:10.3390/s16071119.

[13] Dan Mihai Ştefănescu. *Wheatstone Bridge - The Basic Circuit for Strain Gauge Force Transducers*, pages 347–360. Springer Berlin Heidelberg, Berlin, Heidelberg, 2011. URL: https://doi.org/10.1007/978-3-642-18296-9_18, doi:10.1007/978-3-642-18296-9_18.

[14] Carlo Massaroni, Paola Saccomandi, and Emiliano Schena. Medical smart textiles based on fiber optic technology: An overview. *Journal of Functional Biomaterials*, 6(2):204–221, 2015. URL: https://dx.doi.org/10.3390/jfb6020204, doi:10.3390/jfb6020204.

[15] Thomas Publishing Company. All about force sensors, 2023. Accessed on January 08, 2023. URL: https://www.thomasnet.com/articles/instruments-controls/all-about-force-sensors/.

[16] OHMITE, Warenville, IL, USA. *Integration Guide Force Sensing Resistor*, 1st edition, 2018.

[17] Edwin Dertien Paul Regtien. *Sensors for Mechatronics*. Elsevier, Amsterdam, 2 edition, 2018. doi:https://doi.org/10.1016/B978-0-12-813810-6.00001-X.

[18] Paul Regtien. *Electronic instrumentation*. VSSD, Delft, 2 edition, 2005.

[19] Fluke Corporation. Why is calibration important?, 2022. Accessed on January 27, 2023. URL: https://us.flukecal.com/why-is-calibration-important.

[20] Alexandre Martins, José Torres Farinha, and Antonio J. Marques Cardoso. Calibration and certification of industrial sensors – a global review. *WSEAS TRANSACTIONS ON SYSTEMS AND CONTROL*, 2020.

[21] J. A. Flórez and A. Velásquez. Calibration of force sensing resistors (fsr) for static and dynamic applications. In *2010 IEEE ANDESCON*, pages 1–6, 2010. doi:10.1109/ANDESCON.2010.5633120.

[22] Elprocus. Uart communication : Block diagram and its applications, 2013. Accessed on June 25, 2023. URL: https://www.elprocus.com/basics-of-uart-communication-block-diagram-applications/.